© 2019. Published by The Company of Biologists Ltd | Journal of Cell Science (2019) 132, jcs231506. doi:10.1242/jcs.231506

RESEARCH ARTICLE

FKBP52 regulates TRPC3-dependent Ca^{2+} signals and the hypertrophic growth of cardiomyocyte cultures

Sandra Bandleon[1], Patrick P. Strunz[1], Simone Pickel[2], Oleksandra Tiapko[3], Antonella Cellini[1], Erick Miranda-Laferte[2] and Petra Eder-Negrin[1,*]

ABSTRACT

The transient receptor potential (TRP; C-classical, TRPC) channel TRPC3 allows a cation (Na^+/Ca^{2+}) influx that is favored by the stimulation of G_q protein-coupled receptors (GPCRs). An enhanced TRPC3 activity is related to adverse effects, including pathological hypertrophy in chronic cardiac disease states. In the present study, we identified FK506-binding protein 52 (FKBP52, also known as FKBP4) as a novel interaction partner of TRPC3 in the heart. FKBP52 was recovered from a cardiac cDNA library by a C-terminal TRPC3 fragment (amino acids 742–848) in a yeast two-hybrid screen. Downregulation of FKBP52 promoted a TRPC3-dependent hypertrophic response in neonatal rat cardiomyocytes (NRCs). A similar effect was achieved by overexpressing peptidyl-prolyl isomerase (PPIase)-deficient FKBP52 mutants. Mechanistically, expression of the FKBP52 truncation mutants elevated TRPC3-mediated currents and Ca^{2+} fluxes, and the activation of calcineurin and the nuclear factor of activated T-cells in NRCs. Our data demonstrate that FKBP52 associates with TRPC3 via an as-yet-undescribed binding site in the C-terminus of TRPC3 and modulates TRPC3-dependent Ca^{2+} signals in a PPIase-dependent manner. This functional interaction might be crucial for limiting TRPC3-dependent signaling during chronic hypertrophic stimulation.

KEY WORDS: TRPC3, FKBP, Calcineurin, Calcium, Cardiomyocyte

INTRODUCTION

The transient receptor potential (TRP; C-classical, TRPC) channels are tetrameric, non-selective ion channels in the plasma membrane of mammalian cells that are assembled by seven possible subunits (TRPC1–TRPC7, *TRPC2* is as pseudogene in humans) (Ramsey et al., 2006). As immediate downstream targets of the G_q protein-coupled receptor (GPCR) signaling pathway, they are implicated in a wide range of cellular events in different tissues and organs (Ramsey et al., 2006). Especially in the heart, the stimulation of GPCRs increases a TRPC-mediated Ca^{2+} influx that activates Ca^{2+}-sensitive maladaptive signaling pathways in pathological stress conditions during chronic pressure overload induction or myocardial infarction injury (Eder, 2017; Eder and Molkentin, 2011; Freichel et al., 2017).

[1]Comprehensive Heart Failure Center Wuerzburg, The Department of Internal Medicine I, University Hospital Wuerzburg, Am Schwarzenberg 15, 97078 Wuerzburg, Germany. [2]Institute of Physiology, University of Wuerzburg, Röntgenring 9, 97070 Wuerzburg, Germany. [3]Gottfried Schatz Research Center for Cell Signaling, Metabolism and Aging, Medical University of Graz, 8010 Graz, Austria.

*Author for correspondence (eder_p@ukw.de)

P.E., 0000-0002-6072-8963

Received 6 March 2019; Accepted 11 September 2019

A single TRPC subunit is composed of six transmembrane domains with a pore-forming loop connecting the transmembrane domains 5 and 6, a preserved 25 amino acid sequence called a 'TRP' domain and two cytosolic domains, an N-terminal ankyrin repeat domain and a C-terminal coiled-coil domain (Eder et al., 2007; Fan et al., 2018). The cytosolic domains mediate ion channel formation and are implicated in ion channel regulation and plasma membrane targeting (Eder et al., 2007). Among several protein interaction sites, the C-terminus of all TRPC subunits harbors a highly conserved proline-rich sequence that corresponds to the binding domain in the *Drosophila* photoreceptor channel TRPL for the FK506-binding protein 59 (dFKBP59; LPPPFNVLPSVK) (Sinkins et al., 2004; Vazquez et al., 2004), the *Drosophila* homolog of human FKBP52 (also known as FKBP4). The functionally and structurally related subunits TRPC3, TRPC6 and TRPC7 preferably interact with the FKBP isoform FKBP12 (also known as FKBP1A), and the subunits TRPC1, TRPC4 and TRPC5 with FKBP52 (Sinkins et al., 2004).

Both FKBP12 and FKBP52 are cytosolic proteins that bind the immunosuppressive drug FK506 and function as *cis*/*trans* isomerases (Bonner and Boulianne, 2017). The isomerase activity is mediated by a peptidyl-prolyl *cis*/*trans* isomerase (PPIase) site that binds and stabilizes peptidyl-prolyl (PP) bonds in sterically and electrically favorable positions (Lehnart et al., 2003). Also, the activity of TRPC channels is regulated in an isomerase-dependent fashion (Shim et al., 2009). Owing to their close resemblance to X-prolyl dipeptides, FK506 disrupts the association between FKBP proteins and their target proteins (Ivery, 2000). Independently of this ability, FK506 exerts immunosuppressive effects by building complexes with FKBP12, which results in the inhibition of calcineurin (Martínez-Martínez and Redondo, 2004). This function is confined to small FKBP proteins but not to the high molecular mass FKBP52 (Erlejman et al., 2014). FKBP52 is mainly known as a co-chaperone in heat shock protein 90 (Hsp90)–steroid receptor complexes (Erlejman et al., 2014) and shows a more complex architecture: it contains a catalytic FKBP12-like domain 1 (FK1), including a PPIase site and an FK506-binding pocket, a second PPIase like domain 2 (FK2) without catalytic activity, a domain of three tetratricopeptide (TPR) repeats and a C-terminal calmodulin (CaM)-binding site (Erlejman et al., 2014). The regulation of steroid receptors is dependent on this structural organization. TPR regions in FKBP52 mediate the association with Hsp90 while the FK1 domain in FKBP52 increases receptor transactivation (Sivils et al., 2011) through its isomerase activity.

In the present study, we searched for novel modulators and interaction partners of TRPC channels in the heart. We focused on TRPC3 as one of the most relevant isoforms in the maladaptive hypertrophic program during chronic disease states (Kiyonaka et al., 2009; Nakayama et al., 2006; Wu et al., 2010; Zhang et al., 2018). We identified FKBP52 as a direct interaction partner of TRPC3, which supports the hypothesis of more promiscuous interactions

Journal of Cell Science (2019) 132, jcs231506. doi:10.1242/jcs.231506

between TRPC channels and FKBP proteins. As another novel aspect, we found that an association with FKBP52 is mediated by a C-terminal region of TRPC3 outside the putative immunophilin-binding region in TRPC3. Our functional analyses further demonstrated that the overexpression of FKBP52 truncation mutants lacking the functional PPIase domain enhanced TRPC3 currents and Ca^{2+} fluxes. In cardiomyocytes, this increase in TRPC3 activity was coupled to an enhanced hypertrophic signaling.

RESULTS

TRPC3 associates with FKBP52 through a distal C-terminal region

To identify novel interaction partners of TRPC3 in the heart, we performed a yeast two-hybrid screen known as a Ras recruitment system, which is based on the restoration of the Ras signaling transduction pathway in yeast (Aronheim, 2004; Kehat et al., 2011). As baits, we used the cytosolic regions of human TRPC3 (accession no. Q13507): an N-terminal protein fragment including the amino acids (aa) 1–341 and two C-terminal fragments covering the proximal (aa 670–797) and the distal C-terminal region (aa 742–848; marked as red bars in Fig. 1A) of TRPC3. The mouse cardiac cDNA library was composed of cDNAs fused to a myristoylation factor which allowed anchorage of the proteins to the cell membrane and interaction with the respective baits in the cytoplasm. With both the N-terminus aa 1–341 and the C-terminal region aa 742–848, positive clones from the cDNA library were recovered (Table 1). The C-terminal region aa 670–797 did not reveal any protein–protein interactions. There were 20–40 repetitive colonies expressing the myosin light chain-related proteins, myosin light chain regulatory B-like and myosin light chain polypeptide 2, as well as the triosephosphate isomerase, which we considered as non-specific interactions and thus did not include in subsequent investigations. We also found colonies expressing the sarcomeric proteins desmin and myomesin; however, we could not validate their interactions with TRPC3 in co-immunoprecipitation (co-IP) studies. The recovery of several mitochondrial proteins in the screen was a surprising finding, which could a set a basis for more detailed analyses to elucidate the mitochondrial aspect of TRPC3-dependent Ca^{2+} signaling. There was an interaction with the pre-B-cell leukemia transcription factor interacting protein, an as yet undescribed transcription factor in the heart. Among these candidates, the immunophilin FKBP52 (accession no. NM_010219) appeared as physiologically relevant interaction partner of TRPC3 given its established role as co-chaperone and ion channel regulator. Another rationale for continuing to analyze the TRPC3–FKBP52 interaction was the fact that FKBP52 bound to the C-terminal region aa 742–848 (Fig. 1B), which is beyond the putative FKBP-binding motif (proline-rich region PP, Fig. 1A), a region that is common in all TRPC isoforms.

FKBP52 is composed of an N-terminal FK1 domain with a PPIase active site and an FK506-binding region, an FK2 domain without isomerase activity followed by three TPR1-3 repeats, and a C-terminal CaM-binding site (Fig. 1C). The FKBP52 cDNA clone from the yeast two-hybrid screen covered the sequence aa 135–459, including the FK2 domain (aa 167–253), the regions TPR1 (aa 270–303), TPR2 (aa 319–352), TPR3 (aa 353–386) and the C-terminus (Fig. 1C; Fig. S1). The sequence did not contain the isomerase domain FK1 (aa 50–138), except for three amino acids (aa 135–138). Sequence alignment revealed a single point mutation at G1075A, resulting in an amino acid change of R358Q in the TPR3 region of the FKBP52 clone (Fig. 1C; Fig. S1). In co-IP studies, we further analyzed this interaction between the FKBP52 fragment (aa 135–459) from the yeast two-hybrid screen and TRPC3. Confirming the results from the screen, TRPC3 was detected in the immunocomplex of precipitated hemagglutinin (HA)-tagged FKBP52 (aa 135–459; Fig. 1D). This interaction was comparable to the binding between endogenously expressed FKBP52 and YFP–TRPC3 in HEK 293 cells and in homogenates from mouse hearts (Fig. 1E,F). These results indicate that FKBP52 directly interacts with TRPC3 via a non-classical FKBP region in the C-terminus of TRPC3.

Mapping of FKBP52 protein sequences involved in FKBP52–TRPC3 binding

Next, we analyzed which protein structures in FKBP52 mediate the interaction with TRPC3. We constructed five, N-terminally HA-tagged FKBP52 cDNAs covering the following FKBP52 regions: aa 1–138 (PPIase/FK506 domain); aa 139–253 (FK2 domain); aa 230–303 (FK2 and TPR1); aa 280–352 (TPR1 and TPR2); aa 352-459 (TPR3 with the R358Q mutation; marked as red asterisk) and the C-terminal region of FKBP52 (Fig. 2A). Then we performed co-IP studies in HEK 293 cells co-expressing YFP–TRPC3 and each of the HA-tagged FKBP52 protein domains by using an HA-antibody. Our co-IP data showed an interaction between TRPC3 and the FKBP52 fragments aa 1–138, aa 139–253, aa 230–303 and aa 280–352. The C-terminal region of FKBP52 (aa 352–459) containing the mutated TPR3 site and the CaM-binding site did not interact with TRPC3 (Fig. 2B,C). This lack of interaction was still observed after back-mutating the FKBP52 fragment (aa 352–459) with the R358Q mutation to wild-type FKBP52 (Fig. 2D). Based on these data, several regions of FKBP52 associate with TRPC3, including the FK1, FK2, TPR1 and TPR2 domains. TPR3 and the C-terminal domain do not interact with TRPC3.

FKBP52 is linked to TRPC3-dependent hypertrophic effects in neonatal rat cardiomyocytes

TRPC3 has been suggested to be an important determinant in cardiomyocyte function and Ca^{2+}-dependent signaling mechanisms in the pathological hypertrophic growth of the heart (Eder, 2017; Eder and Molkentin, 2011). We therefore started experiments to analyze whether the pro-hypertrophic effects of TRPC3 were dependent on FKBP52. In a first step, we assessed the hypertrophic growth of cultures from neonatal rat cardiomyocytes (NRCs) treated with FKBP52 siRNAs (Fig. 3A) and with the TRPC3 inhibitor pyrazole 3 (Pyr3) (Kiyonaka et al., 2009). In an agonist-dependent approach, we stimulated the cells with the GPCR agonist phenylephrine (PE) for 24 h. As shown in Fig. 3B,C, PE stimulation resulted in a ∼30% enlargement of cardiomyocytes, which was significantly enhanced when FKBP52 was downregulated. When we treated the cells with the TRPC3 inhibitor Pyr3, we found that the hypertrophic increase in scramble (Scr) siRNA-treated cells was not affected. In contrast, cardiomyocytes with downregulated FKBP52 expression levels showed a significantly reduced cell size when treated with Pyr3, which was noticeable both at baseline as well as after PE stimulation. These results indicate that an inhibition of TRPC3 attenuates hypertrophy, provided that FKBP52 expression levels are lowered in cardiomyocytes. TRPC6, the structurally and functionally related isoform of TRPC3 was also affected by a downregulation of FKBP52. Hence, overexpression of TRPC6 in NRCs caused a significant baseline hypertrophy, which under PE-stimulatory conditions was elevated when FKBP52 was downregulated (Fig. S2). These results indicate that there is a functional association not only between FKBP52 and TRPC3 but also with TRPC6, which could take place either through a direct binding

Journal of Cell Science (2019) 132, jcs231506. doi:10.1242/jcs.231506

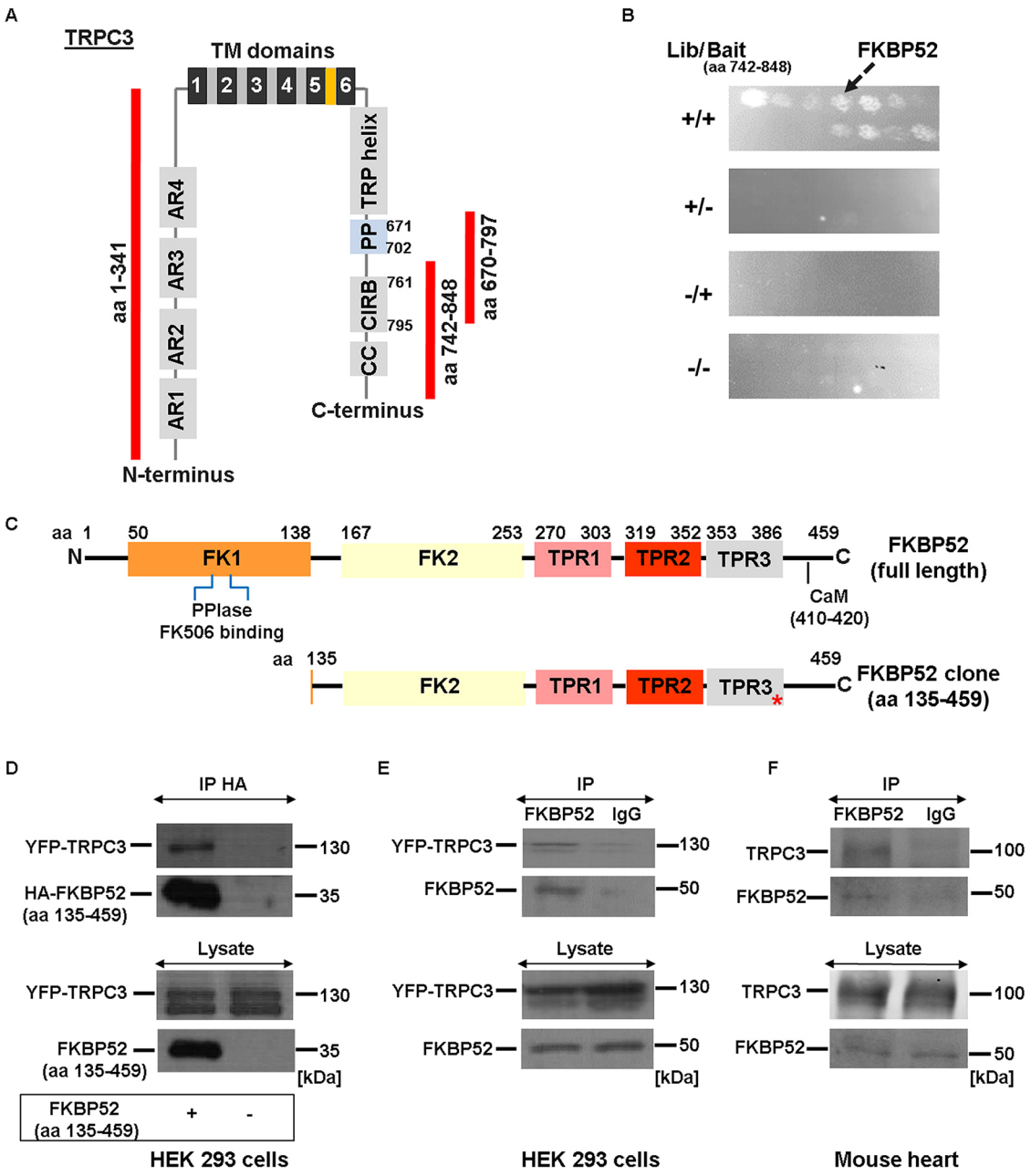

Fig. 1. FKBP52 identified as novel interaction partner of TRPC3 in the heart. (A) Diagram of a single TRPC3 subunit and its structural organization. Shown are the N-terminus with ankyrin repeats 1–4 (AK1–4), 6 transmembrane (TM) domains with the pore region marked in yellow and the C-terminus with a TRP helix, proline-rich (PP) region, calmodulin/IP_3 receptor-binding (CIRB) and a coiled-coil (CC) domain. The red bars indicate the protein fragments (aa 1–341, 670–797 and 742–848) used as baits in the Ras recruitment yeast two-hybrid screen. (B) A yeast two-hybrid growth assay with the C-terminal TRPC3 protein fragment aa 742–848 revealed the immunophilin FKBP52 as a direct interaction partner of TRPC3. Yeast cells were co-transfected with TRPC3 [aa 742–848 (bait)] and a cardiac mouse cDNA library as prey (Lib). Cells were grown on selective media to induce the expression of Lib and bait (+/+), Lib (+/–; negative control), bait (–/+; negative control), or neither Lib nor bait (–/–), respectively. Growth of the cells expressing Lib and bait (+/+) reflects a direct protein–protein interaction. (C) Diagram of FKBP52. FK1 (aa 50–138) comprises the PPIase domain and FK506-binding pocket, which is followed by FK2 (aa 167–253), three TPR repeats (TPR1, aa 270–303; TPR2, aa 319–352; and TPR3, aa 353–386) and a C-terminus with a CaM-binding site. Note the shortage of the FK1 domain and the point mutation (R358Q; marked as red asterisk) in the FKBP52 protein found in the yeast two-hybrid screen. (D) HEK 293 cells were transfected with the HA-tagged FKBP52 fragment (aa 135–459) or vector control (HA-pcDNA3.1) together with YFP–TRPC3 to immunoprecipitate HA–FKBP52 (aa 135–459) and detect YFP–TRPC3 or HA–FKBP52, respectively. (E) Interaction between YFP–TRPC3 and natively expressed FKBP52, as confirmed by IP of FKBP52 or control IgG and consecutive detection of YFP–TRPC3 in HEK 293 cells. (F) Co-IP of FKBP52 and TRPC3 in mouse cardiac lysates. D–F show representative western blots from three independent experiments.

between FKBP52 and TRPC6 or indirectly through the heteromerization between TRPC3 and TRPC6, a common feature described in several cell types (Dietrich et al., 2005; Strübing et al., 2003; Wu et al., 2010).

The pro-hypertrophic phenotype of NRCs induced by a downregulation of FKBP52 could also be based on mechanisms other than TRPC channel regulation. Hypertrophy will involve a re-arrangement of the cytoskeletal network, which includes the

Journal of Cell Science (2019) 132, jcs231506. doi:10.1242/jcs.231506

Table 1. Clones from a cardiac mouse cDNA library recovered with either the N-terminus (aa 1–341) or the C-terminal fragment (aa 742–848) of TRPC3 in a Ras recruitment yeast two-hybrid screen

Protein interactions with the N-terminus (aa 1–341) of TRPC3
Myosin light chain regulatory B like
Myosin light chain polypeptide 2
Desmin
Myomesin
Creatine kinase, mitochondrial sarcomeric
Mitochondrial aconitase
Translocase of inner mitochondrial membrane 44
Triosephosphate isomerase
Protein interactions with the C-terminus (aa 742–848) of TRPC3
FKBP52
Myosin light chain polypeptide 2
Pre-B-cell leukemia transcription factor interacting protein 1
Triosephosphate isomerase

stabilization of microtubules. As FKBP52 might play an integral part in microtubule formation (Chambraud et al., 2007), we examined cytoskeletal fractions of NRCs after 24 h of PE stimulation (Fig. S3). Stabilized microtubules are characterized by an increased detyrosination of α-tubulin, which results in the removal of the C-terminal leaving a glutamine on the C-terminus (Glu-tubulin) (Fassett et al., 2009). Western blotting of cytoskeletal extracts showed that PE stimulation indeed resulted in increased Glu-tubulin expression levels, however, with no significant differences between Scr and FKBP52 siRNA-treated NRCs (Fig. S3).

Overexpression of FKBP52 truncation mutants promotes cardiomyocyte hypertrophy and calcineurin/NFAT signaling

Analogous to what is seen for steroid receptors (Sivils et al., 2011), the regulation of TRPC3 by FKBP52 might be mediated through several different regions of FKBP52. Thus, TPR domains might be involved in the physical association with TRPC3, and the functional PPIase domain in FKBP52 might modulate TRPC3 activity and related hypertrophic mechanisms. Following this hypothesis, we expressed PPIase-deficient structural FKBP52 fragments in order to examine hypertrophy and signaling mechanisms in NRCs. In a first attempt, we infected NRCs with adenoviruses encoding the FKBP52 fragment FKBP52 (aa 135–459) or β-galactosidase (βgal) as control. We then stimulated the cells with PE or the diacylglycerol analogue 1-oleoyl-2-acetyl-*sn*-glycerol (OAG), which is a well-established direct activator of TRPC3 (Tiapko and Groschner, 2018). In both conditions, the hypertrophic enlargement was significantly elevated by FKBP52 (aa 135-459; Fig. 4A,B). Treating NRCs with Pyr3 reversed the pro-hypertrophic effect of FKBP52 (aa 135–459) during stimulation. Notably, adult cardiomyocytes responded with a comparable phenotype, which was characterized by an FKBP52 (aa 135–459)-dependent hypertrophic enlargement induced by the stimulation with PE for 24 h (Fig. 4C,D).

To obtain a broader view of GPCR signaling cascades that are mechanistically connected with TRPC3, we examined NRCs after angiotensin II (Ang II) stimulation. Under these stimulatory conditions, FKBP52 (aa 135-459) also promoted the hypertrophic response (Fig. S4A), which was linked to a slight increase in the expression levels of the hypertrophic marker atrial natriuretic peptide (ANP; Fig. S4B). Interestingly, treatment of NRCs with the immunosuppressant agent FK506 resulted in opposite effects with slightly decreased ANP levels in NRCs (Fig. S4C).

In a next step, we examined potential mechanisms that are involved in FKBP52–TRPC3 cardiomyocyte signaling. First, we analyzed the activation of the nuclear factor of activated T-cells (NFAT) isoform NFATc1 by quantifying its relative localization in the cytosol and nucleus of NRCs. There was an increased nuclear localization of NFATc1–GFP in cells overexpressing FKBP52 (aa 135–459; Fig. 5A,B) or the shorter structural fragment FKBP52 (aa 280–352; Fig. 5C,D). This increased nuclear localization was noticeable at the baseline and was reversed by treating the cells with Pyr3. An acute stimulation with the GPCR agonists Ang II or PE did not further promote the activity of NFATc1 (Fig. S5A), a phenomenon that was previously described in rabbit cardiomyocytes (Rinne et al., 2010). Thus, to analyze whether the structural FKBP52 fragments FKBP52 (aa 135–459) and FKBP52 (aa 280–352) also affected calcineurin signaling under stimulatory conditions, we analyzed mRNA levels of the regulator of calcineurin 1 (also known as calcipressin-1; *RCAN1*) and protein expression levels of NFATc3, a repeatedly described downstream target of TRPC channels (He et al., 2017; Kuwahara et al., 2006). Interestingly, *RCAN1* was barely upregulated in control-infected NRCs after 24 h of Ang II stimulation, but significantly increased in FKBP52 (aa 135–459)-infected cardiomyocytes (Fig. S5B). To evaluate the effects of FKBP52 (aa 135–459) on NFATc3 expression levels, we isolated nuclear fractions from NRCs. In contrast to what was found for NFATc1, NFATc3 was activated during GPCR stimulation with PE, as evidenced by an increased expression of NFATc3 in the nucleus of βgal-infected NRCs and an even further elevation in cells expressing FKBP52 (aa 135–459; Fig. 5E,F).

Based on these data, FKBP52 (aa 135-459) affects calcineurin/NFAT signaling both at baseline and after GPCR stimulation, but cardiomyocyte hypertrophy only under stimulatory conditions. We therefore hypothesized whether the baseline NFAT activity was not sufficient to induce hypertrophy and requires further transcriptional regulators that become activated during GPCR stimulation. We analyzed the expression of the histone deacetylase 4 (HDAC4), a downstream target of the Ca^{2+}/calmodulin-dependent protein kinase II (CamKII), a Ca^{2+}-sensitive regulator of hypertrophy (Backs et al., 2006). Phosphorylation of HDAC4 by CaMKII results in the nuclear export of HDAC4 and a re-expression of genes driving cardiomyocyte hypertrophy (Backs et al., 2006). We found slightly decreased expression levels of HDAC4 in nuclear fractions from cells overexpressing FKBP52 (aa 135–459) after PE stimulation and, vice versa, increased HDAC4 expression levels in the cytosol (Fig. 5G,H). This adaption might contribute to the hypertrophic profile of cardiomyocytes with elevated FKBP52 (aa 135–459) expression levels.

FKBP52 affects TRPC3-mediated Ca^{2+} signals and ion channel activity

To test the hypothesis that the functional interaction between FKBP52 and TRPC3 regulates the observed hypertrophic events in cardiomyocytes, we measured cytosolic Ca^{2+} signals in NCRs and HEK 293 cells by applying OAG as TRPC3 activator. In comparison to βgal-infected cells, we found an increased Ca^{2+} influx in cells overexpressing either FKBP52 (aa 135–459) or FKBP52 (aa 280–352; Fig. 6A). Pre-treating the cells with Pyr3 significantly reduced OAG-dependent Ca^{2+} signals (Fig. 6B). The functional link between TRPC3 and FKBP52 was also noticeable in HEK 293 cells. Comparable to the situation in NRCs, TRPC3-mediated Ca^{2+} signals were increased in the presence of FKBP52 (aa 280–352; Fig. 6C,D). In addition, Fura 2-AM experiments in a TRPC3 cell line with downregulated FKBP52 expression levels

Journal of Cell Science (2019) 132, jcs231506. doi:10.1242/jcs.231506

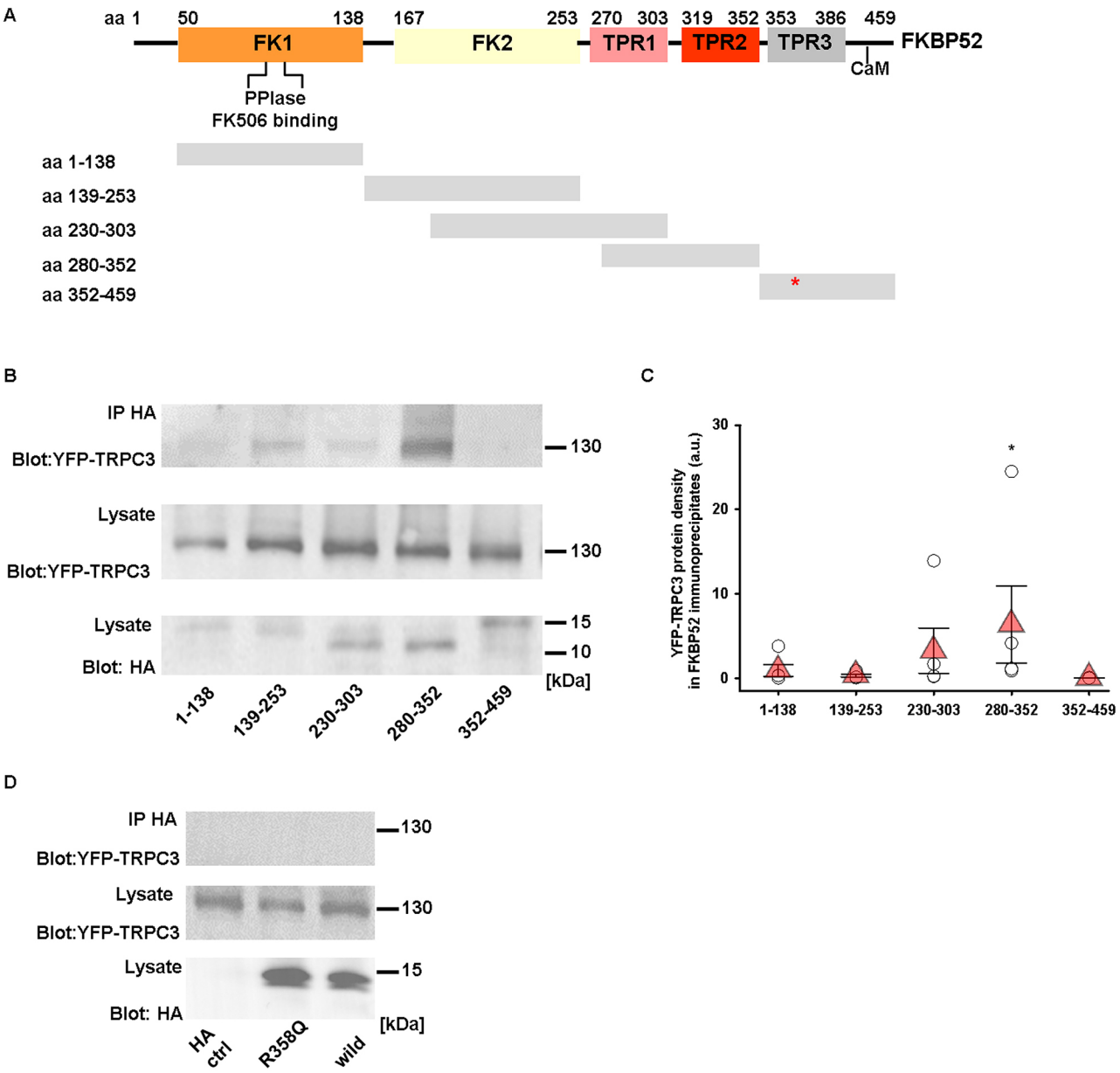

Fig. 2. Identification of FKBP52 sequences involved in FKBP52-TRPC3 binding. (A) Protein structure of FKBP52 with corresponding protein fragments used for co-IP studies in HEK 293 cells. Domains shown are FK1, which contains the with the PPIase and FK506-binding pocket; FK2, three tetratricopeptide (TPR) repeats (TPR1–3), and a C-terminus with a CaM-binding site. The red asterisk marks the location of the point mutation R358Q in FKBP52. (B) HA-tagged FKBP52 protein fragments aa 1–138, 139–253, 230–303, 280–352 and 352–459 were expressed together with YFP–TRPC3 in HEK 293 cells. Immunoblots were probed with anti-YFP or anti-HA antibodies, respectively. (C) Protein levels of YFP–TRPC3 after co-IP with different HA-tagged FKBP52 fragments. *P<0.05 versus 352–459 (Analysis of Variance on Ranks followed by the Dunn's Method), n=5, mean±s.e.m. (D) Co-IP of YFP–TRPC3 in lysates from HEK 293 cells expressing YFP–TRPC3 together with HA–FKBP52 (aa 352–459), including the mutation R358Q, wild-type HA–FKBP52 (aa 352–459; wild) or HA vector control (HA ctrl). An anti-HA antibody was used for the IP. B and D show blots that are representative of three independent experiments.

showed the same trend (Fig. S6A,B). In that case, stimulation of TRPC3 with the GPCR agonist carbachol resulted in a TRPC3-mediated Ca^{2+} influx, which was further increased when FKBP52 was downregulated.

In order to gain insight into more direct effects on TRPC3 function, we measured the activity of TRPC3 channels in whole-cell patch-clamp analyses. We transfected HEK 293 cells with YFP–TRPC3, YFP–TRPC3+FKBP52 (aa 280–352) or a YFP-encoding plasmid and elicited TRPC3-mediated currents with OAG (Tiapko and Groschner, 2018). As shown in Fig. 6, the addition of OAG resulted in a profound increase in current densities in HEK 293 cells expressing YFP–TRPC3 and an even further increase when FKBP52 (aa 280–352) was co-expressed. Co-expression of full-length FKBP52 reversed the stimulatory effect of FKBP52 (aa 280–352; Fig. 6E,F).

FKBP52 truncation mutants do not strengthen the association of TRPC3 with calcineurin, Homer1 or FKBP12

Besides a functional crosstalk, we also considered the possibility of FKBP52 physically interfering with an interaction between TRPC3 and calcineurin. We were interested to find out whether the increased calcineurin activity was based on a tighter association

Journal of Cell Science (2019) 132, jcs231506. doi:10.1242/jcs.231506

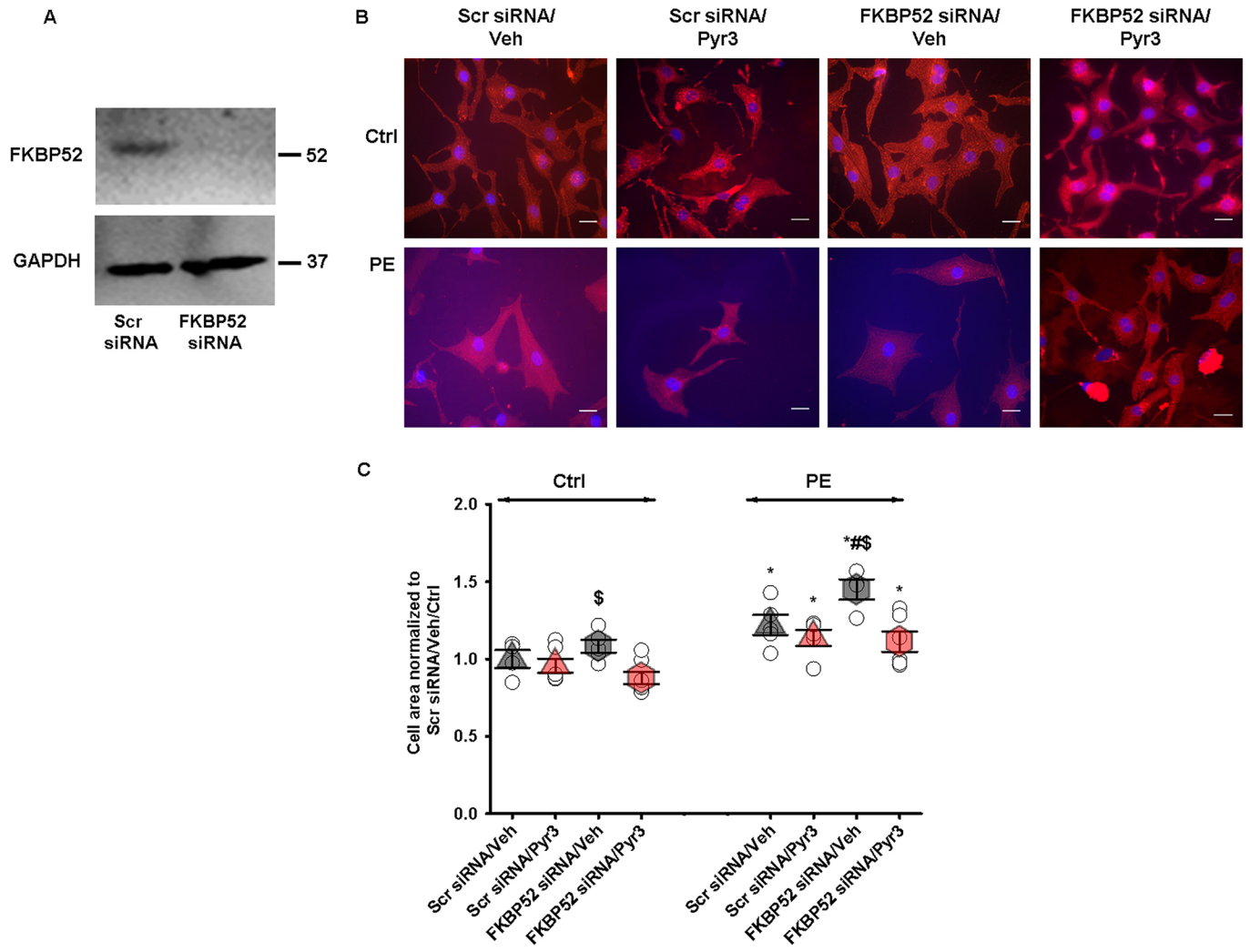

Fig. 3. Inhibition of TRPC3 attenuates cardiomyocyte hypertrophy induced by a downregulation of FKBP52. (A) NRCs were transfected with FKBP52 (FKBP52 siRNA) or scramble siRNAs (Scr siRNA). Confirmation of FKBP52 silencing as shown by western blotting. (B) The hypertrophic growth of NRCs was measured as an increase of the area of the cell surface after PE (50 µM) or control (Ctrl) treatment for 24 h. Cells were treated with FKBP52 siRNA or Scr siRNA with 10 µM Pyr3 or vehicle (Veh). Red, α-actinin; blue, DAPI. Scale bars: 20 µm. Taken with a 63× magnification objective. (C) Quantification of the cell area relative to that in Scr siRNA/Veh/Ctrl. **P*<0.05 versus respective Ctrl stimulation, $^{\#}P$<0.05 versus Scr siRNA/Veh/PE, $^{\$}P$<0.05 versus FKBP52 siRNA/Pyr3/Ctrl or PE, respectively (two-way ANOVA with Holm–Sidak method and unpaired *t*-test), *n*=4–7, mean±s.e.m.

between TRPC3 and calcineurin in the presence of FKBP52 (aa 135–459). According to the quantitative analysis of co-IP protein fractions, however, FKBP52 (aa 135–459) did not strengthen the association between TRPC3 and calcineurin (Fig. 7A,B).

Previous studies on TRPC1 have identified overlapping binding regions in the N-terminus and the C-terminal immunophilin-binding region (LPPPFN) of TRPC1 for FKBP52 and the scaffolding protein Homer1 (Shim et al., 2009). Functionally, Homer1 maintains TRPC1 in a closed state and FKBP52 supports an agonist-induced TRPC1 activation (Yuan et al., 2003). Considering such functional constellation, we analyzed whether an interaction between TRPC3 and the PPIase-deficient FKBP52 structural fragments FKBP52 (aa 135–452) and FKBP52 (aa 280–352) resulted in an increased Homer1 binding in form of a negative-feedback mechanism to prevent over-activation of TRPC3. According to co-IP studies, there was a weak interaction between TRPC3 and Homer1 which was not affected by the expression of either FKBP52 fragment (Fig. 7C). As another functionally relevant immunophilin, FKBP12 was suggested to associate with TRPC3 (Sinkins et al., 2004) via the putative immunophilin-binding region located upstream of the region identified in the yeast two-hybrid screen in the present study. Thus, we analyzed whether an interaction between the PPIase-deficient FKBP52 mutants (aa 135–459 and aa 280–352) and TRPC3 resulted in an increased FKBP12 interaction and thus increased TRPC3 activation as observed in electrophysiology and Ca^{2+} analyses (Fig. 6). Interestingly, we could not detect FKBP12 in TRPC3 precipitates regardless of the expression of FKBP52 (aa 135–459) or FKBP52 (aa 280–352; Fig. 7C).

These results suggest that a PPIase deficiency or loss of total FKBP52 elevates the activity of TRPC3 resulting in elevated Ca^{2+} levels, calcineurin activation and cardiomyocyte hypertrophy.

DISCUSSION

The first indications that FKBP proteins act as regulatory components in TRPC signalplexes were obtained by functional and biochemical studies in the *Drosophila* brain. In particular, the homolog of human FKBP52, dFKBP59, was found to alter TRPL ion channel activation through a direct interaction with a

Journal of Cell Science (2019) 132, jcs231506. doi:10.1242/jcs.231506

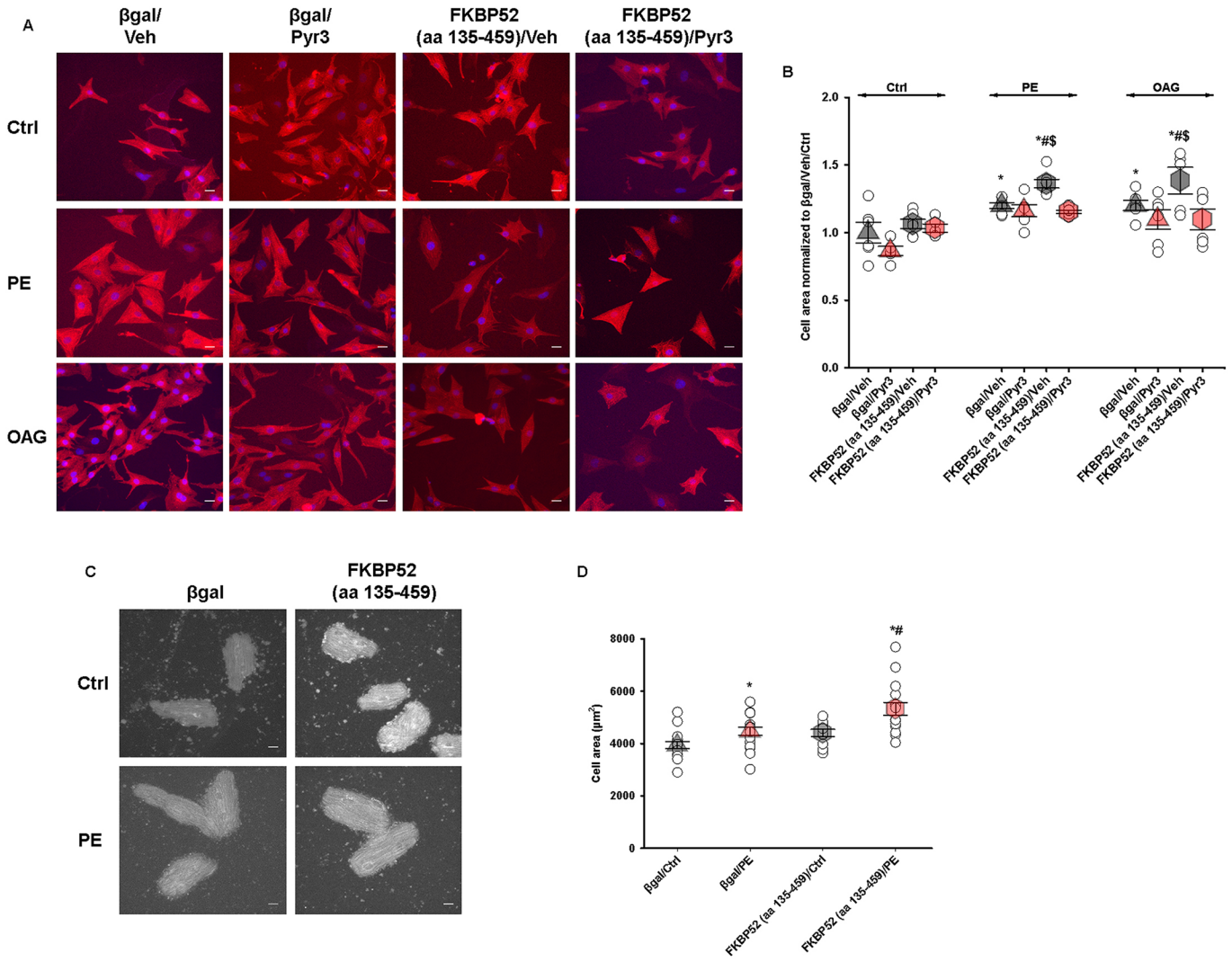

Fig. 4. Overexpression of FKBP52 lacking the functional PPIase site promotes cardiomyocyte hypertrophy. (A) NRCs were infected with adenoviruses encoding βgal or FKBP52 (aa 135–459) and treated with 10 µM Pyr3 or vehicle (Veh). The area of the cell surface, as an indicator of the hypertrophic growth, was analyzed after 24 h of PE (50 µM), OAG (100 µM) or control (Ctrl) stimulation. Red, α-actinin; blue, DAPI. Scale bars: 20 µm. (B) Quantification area of the cell surface relative to βgal-infected controls. **P*<0.05 versus respective control stimulation, $^{\#}$*P*<0.05 versus βgal/Veh/PE or βgal/Veh/OAG, $^{\$}$*P*<0.05 versus FKBP52 (aa 135–459)/Pyr3 (two-way ANOVA with Holm–Sidak method and unpaired *t*-test), *n*=5-7, mean±s.e.m. (C) Adult rat cardiomyocytes infected with βgal or FKBP52 (aa 135–459) and stimulated with PE or without (Ctrl) for 24 h. Scale bar: 20 µm. (D) Quantification area of the cell surface relative to that in to βgal-infected controls. **P*<0.05 versus respective Ctrl stimulation, $^{\#}$*P*<0.05 versus βgal/PE (two-way ANOVA with Holm–Sidak method), *n*=11–17 cells, mean±s.e.m. Images in A and C were taken with a 40× magnification objective.

proline-rich domain in the C-terminus of TRPL (L^{701}PPPENVLP^{709}) (Goel et al., 2001). An almost identical FKBP-binding motif, a proline-rich region (PP) in the C-terminus, is present in all seven mammalian TRPC subunits (Sinkins et al., 2004). The first leucyl-prolyl (LP) bond is conserved among TRPC and TRPL channels, while the second LP bond is changed to a valyl-prolyl (VP) bond in TRPC3, TRPC6 and TRPC7 and to an isoleucyl-prolyl (IP) bond in TRPC1, TRPC4 and TRPC5. Co-IP studies in insect neuronal cells (Sf9) revealed FK506-sensitive interactions between TRPC channels and FKBPs, indicating a role of the C-terminal PP domain as a potential binding motif. Furthermore, it was shown that TRPC1, TRPC4 and TRPC5 bind to FKBP52, whereas TRPC3, TRPC6 and TRPC7 to the small FKBP12 in native brain lysates (Sinkins et al., 2004). The reason for this phenomenon has never been entirely resolved. It has been suggested that the second peptidyl-prolyl (PP) bond determines the FKBP selectivity in a similar fashion to that observed for the regulation of ryanodine receptors (RyRs). RyR2 contains an IP bond that is targeted by FKBP12.6 (also known as FKBP1B) and RyR1 exhibits a VP dipeptide that interacts with FKBP12 (Gaburjakova et al., 2001). However, a swap of peptide bonds in TRPC3 or TRPC5 failed to alter the binding preference for specific FKBP proteins, giving rise to the speculation that additional regions other than the proline-rich domain are implicated in FKBP interactions. Indeed, C-terminal truncations of TRPL showed that an association with FKBP59 was still possible (Goel et al., 2001).

With our data, we confirm the above assumption by demonstrating that a C-terminal region of TRPC3 (aa 742–848) directly interacts with FKBP52. With this finding we also oppose previous suggestions that claim an association between selective TRPC subunits and certain FKBP families (Sinkins et al., 2004). We isolated FKBP52 with a TRPC3 protein fragment that does not

Journal of Cell Science (2019) 132, jcs231506. doi:10.1242/jcs.231506

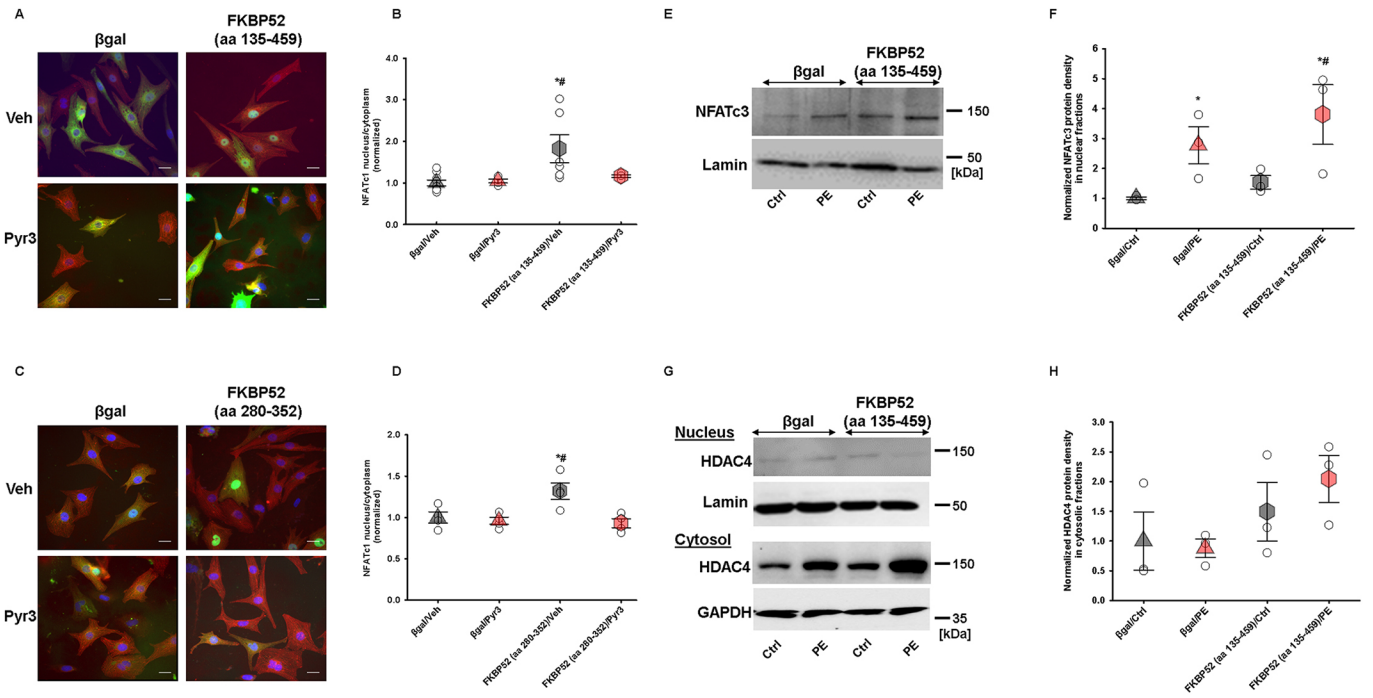

Fig. 5. Overexpression of FKBP52 truncation mutants promotes NFAT signaling. (A) NRCs were co-infected with adenoviruses encoding βgal or FKBP52 (aa 135–459), and NFATc1–GFP (green). Cells were pre-treated with 10 µM Pyr3 or vehicle (Veh). The localization of NFATc1 indicates the state of its activity [in the nucleus (blue) means it is transcriptionally active]. Red, α-actinin. Scale bar: 20 µm. (B) Quantification of the proportion of NFATc1–GFP localized to the nucleus of NRCs. Average quantified values presented relative to that in βgal/Veh. **P*<0.05 versus βgal/Veh, $^{\#}$*P*<0.05 versus FKBP52 (aa 135–459)/Pyr3 (two-way ANOVA with Holm–Sidak method), *n*=4–9, mean±s.e.m. (C,D) NRCs co-infected with adenoviruses encoding βgal or FKBP52 (aa 280–352), and NFATc1–GFP (green). Red, α-actinin; blue, DAPI. Pre-treatment with Pyr3 (10 µM) or Veh. Scale bar: 20 µm. (D) Quantification of the proportion of NFATc1–GFP localized to the nucleus of NRCs. Average quantified values presented relative to that in to βgal/Veh. **P*<0.05 versus βgal/Veh, $^{\#}$*P*<0.05 versus FKBP52 (aa 280-352)/Pyr3 (two-way ANOVA with Holm–Sidak method), *n*=4, mean±s.e.m. (E) Western blot analysis of NFATc3 in nuclear extracts from NRCs overexpressing FKBP52 (aa 135–459) or βgal after 24 h of either 50 µM PE or control (Ctrl) stimulation. (F) Quantification of protein expression levels. **P*<0.05 versus FKBP52 (aa 135–459)/Ctrl, $^{\#}$*P*<0.05 versus βgal/PE (two-way ANOVA with Holm–Sidak method), *n*=3, mean±s.e.m. Lamin was used as loading control. (G) Western blot analysis of HDAC4 in nuclear and cytosolic extracts from NRCs overexpressing FKBP52 (aa 135–459) or βgal after 24 h of either PE or Ctrl stimulation. (H) Quantification of protein expression levels. Differences were not significant (two-way ANOVA with Holm–Sidak method), *n*=3, mean±s.e.m. Lamin and GAPDH were used as loading controls. Images in A and C were taken with a 63× magnification objective.

contain any obvious FKBP-binding motifs. The TRPC3 region aa 742–848 that we used as bait in the yeast two-hybrid screen exhibits CaM/inositol trisphosphate (IP_3)-binding sites and a coiled-coil domain (Trebak et al., 2005) but lacks PP bonds mediating an FKBP-dependent *cis-trans* isomerization. TRPC3 also does not possess the TPR-binding motif (MEEVD) that was found to be required for an association between TPR regions in FKBP52 and heat-shock proteins in steroid receptor complexes (Erlejman et al., 2014). Interestingly, TRPC3 was directly associated with a truncated FKBP52 protein lacking the PPIase site in the FK1 domain (aa 135–459). When we examined potential TRPC3-binding regions in FKBP52 more closely, we found that several FKBP52 regions were bound to TRPC3. This binding pattern is similar to the interaction between FKBP52 and tubulin (Chambraud et al., 2007). In contrast to the tubulin–FKBP52 association, which requires the TPR domains 1–3 as binding regions, the last TPR3 region and the C-terminus of FKBP52 (aa 352–459) failed to interact with TRPC3. This was an unexpected finding since several important binding structures are located in this region including a conserved charge-Y motif in the CaM-binding domain (aa 410–420) and critical residues in TPR3 (K354) (Cheung-Flynn et al., 2003). This lack of interaction was independent of the mutation (R358Q) in FKBP52 (aa 352–459) suggesting a negligible role of this region in TRPC3 binding and a more prominent role of protein–protein interaction sites within TPR1 and TPR2.

By following up the functional relevance of this unique TRPC3–FKBP52 assembly, we found a limiting effect of FKBP52 on TRPC3-dependent Ca^{2+} signals and downstream hypertrophic signaling pathways in cardiomyocytes. These assumptions were corroborated by cytosolic Ca^{2+} measurements in HEK 293 cells that showed increased TRPC3-mediated Ca^{2+} signals under FKBP52 downregulated conditions. In addition, the small structural FKBP52 fragment (aa 280–352), when co-expressed with TRPC3 in HEK 293 cells, elevated an OAG-dependent TRPC3 conductance and Ca^{2+} influx, giving rise to the speculation that an interaction between TRPC3 and FKBP52 (aa 280–352) results in the replacement of endogenously expressed FKBP52 and thus in an alleviation of the inhibitory effect of FKBP52. Further Ca^{2+} studies in NRCs showed that a larger FKBP52 fragment (aa 135–459) had comparable effects on cytosolic Ca^{2+} signals. In line with our observations, *Drosophila* dFKBP59 exerted inhibitory effects on the stimulation and activity of TRPL (Goel et al., 2001). Similarly, it was shown that the open probability of skeletal muscle and cardiac RyRs was reduced by FKBP12 and FKBP12.6, respectively, and the Ca^{2+} sensitivity of the receptors was elevated when FKBP12 or FKBP12.6 were displaced from the receptor (Lehnart et al., 2003). However, in the setting of TRPC channel regulation, FKBP proteins exerted stimulatory effects on ion channel gating. For example, FK506 treatment resulted in a disruption of TRPC6–FKBP12 binding, and decreased the current density and agonist activation of

Journal of Cell Science (2019) 132, jcs231506. doi:10.1242/jcs.231506

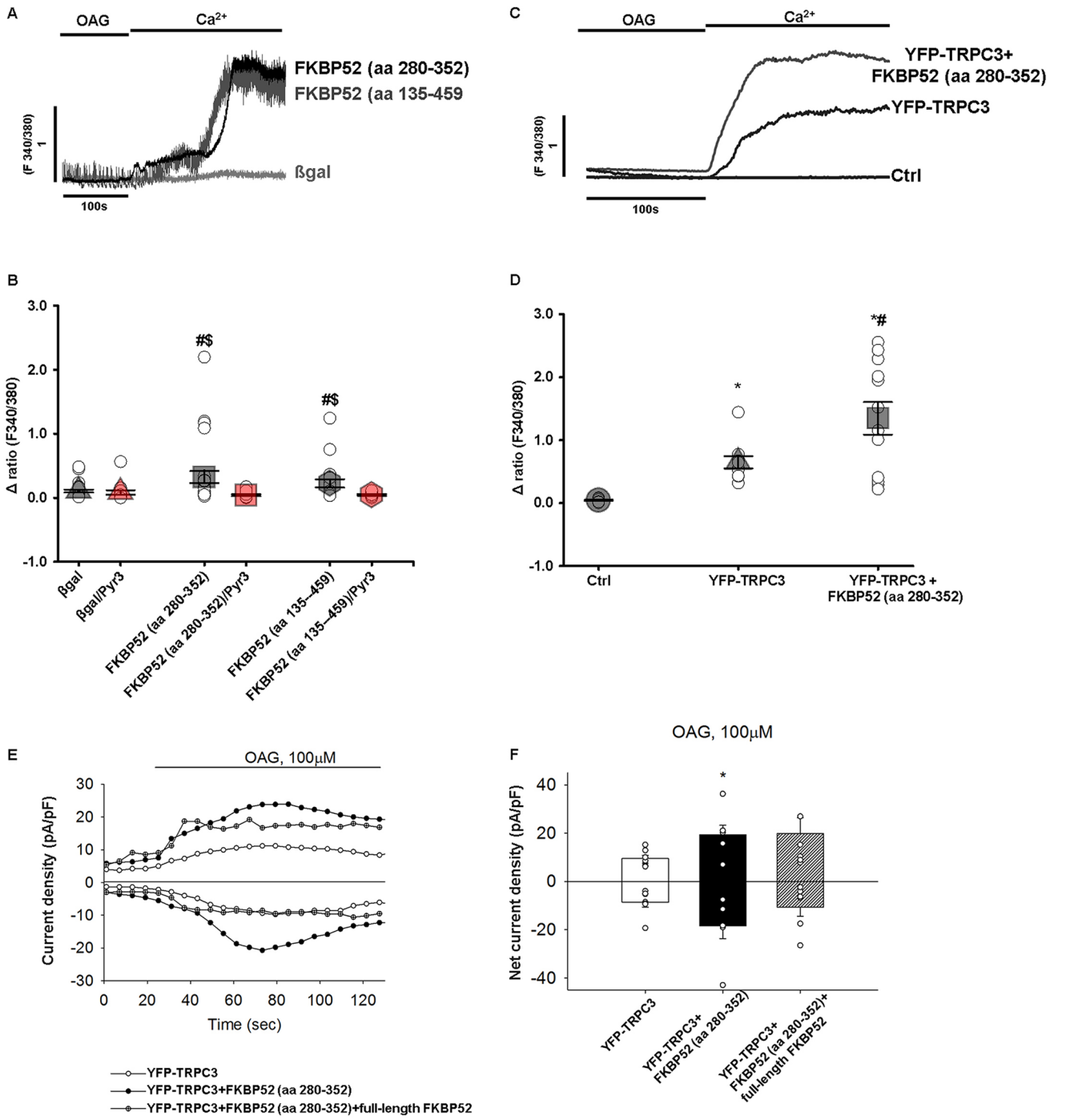

Fig. 6. Altered TRPC3-mediated Ca^{2+} signals and current densities upon expression of FKBP52 truncation mutants. (A) Representative Ca^{2+} recordings in NRCs overexpressing FKBP52 (aa 135–459), FKBP52 (aa 280–352) or βgal using Fura 2-AM. The cells were stimulated with 100 µM OAG in a nominally Ca^{2+}-free Tyrode solution, which was followed by the re-addition of 2 mM Ca^{2+}. Note the increased Ca^{2+} response in the presence of FKBP52 (aa 135–459) and FKBP52 (aa 280–352). (B) Quantification of OAG-induced cytosolic Ca^{2+} signals in NRCs with or without 10 µM Pyr3. Cells overexpressing FKBP52 (aa 135–459), FKBP52 (aa 280–352) or βgal were compared. Mean changes in (Δ) ratio values were calculated by subtracting the peak value after Ca^{2+} re-addition from the baseline value. $^{\#}P$<0.05 versus βgal, $^{\$}P$<0.05 versus FKBP52 (aa 135–459)/Pyr3 or FKBP52 (aa 280–352)/Pyr3, respectively (one-way ANOVA with Holm–Sidak method and unpaired *t*-test), *n*=10–30, mean±s.e.m. (C) Representative Ca^{2+} recordings in HEK 293 cells transfected with YFP–TRPC3, YFP–TRPC3 plus FKBP52 (aa 280–352) or YFP (Ctrl). Stimulation was with 100 µM OAG in a nominally Ca^{2+}-free Tyrode solution and Ca^{2+} re-addition. (D) Quantification of OAG-induced cytosolic Ca^{2+} signals in HEK 293 cells expressing YFP (Ctrl), YFP–TRPC3 or TRPC3 plus FKBP52 (aa 280–352), respectively. Mean Δ ratio values. $^{*}P$<0.05 versus Ctrl, $^{\#}P$<0.05 versus YFP–TRPC3 (one-way ANOVA with Holm–Sidak method), *n*=10–13, mean±s.e.m. (E) Representative time course of the current development in HEK 293 cells transfected with YFP–TRPC3 (white symbols), co-transfected with FKBP52 (aa 280–352; black symbols) or co-transfected with FKBP52 (aa 280–352) and full-length FKBP52 (symbols with crosses) in response to OAG (100 µM). Current values were taken at −90 mV (inward) and at +70 mV (outward). (F) Mean values of the net current in HEK 293 cells expressing YFP–TRPC3 (white), YFP–TRPC3 plus FKBP52 (aa 280–352; black) or YFP–TRPC3 plus FKBP52 (aa 280–352) plus full-length FKBP52 (hatched) in response to OAG. Current values at −90 mV (inward) and at +70 mV (outward) were normalized by cell capacitance and are indicated with circles for each condition. $^{*}P$<0.05 versus YFP–TRPC3 (one-way ANOVA with Holm–Sidak method), mean±s.e.m.

Journal of Cell Science (2019) 132, jcs231506. doi:10.1242/jcs.231506

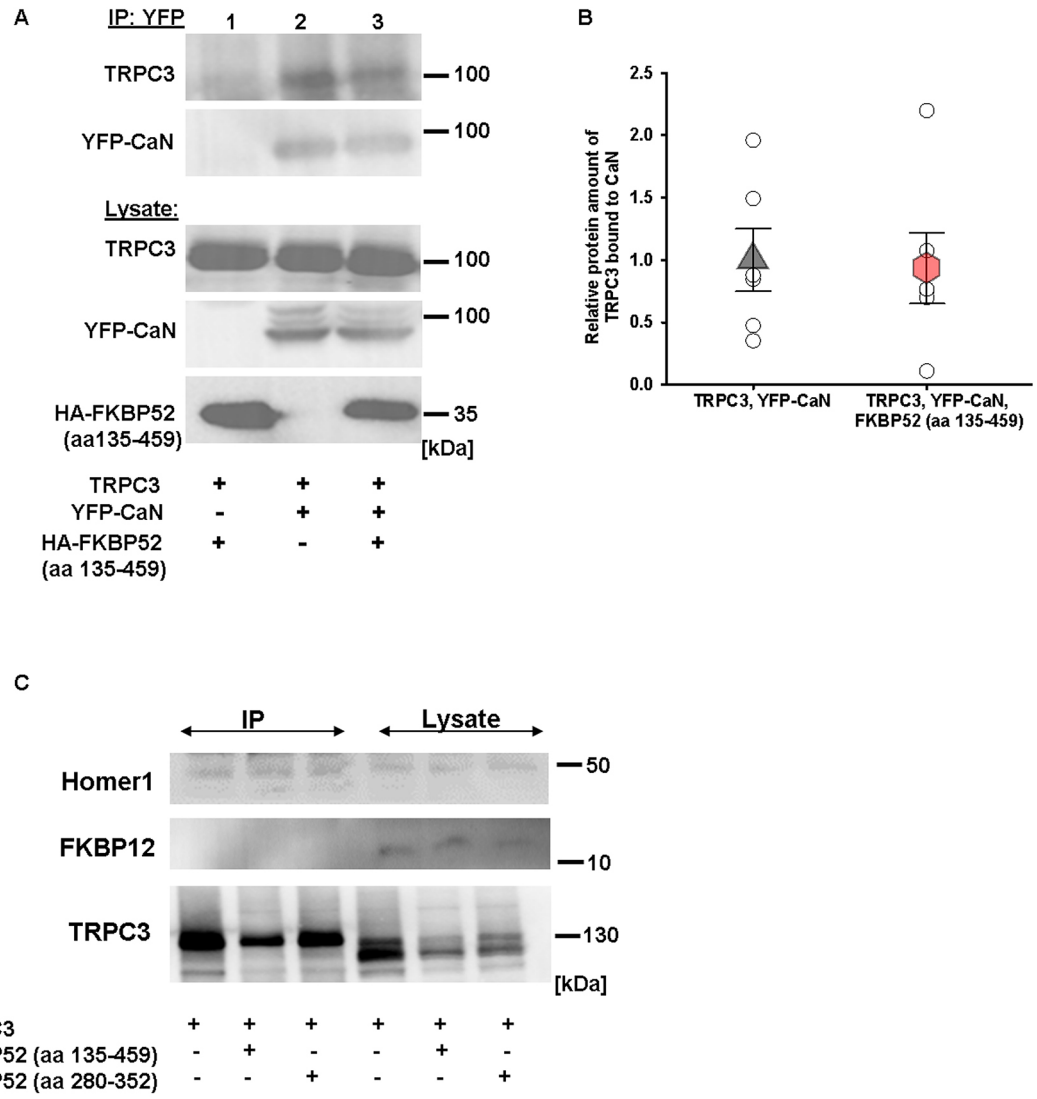

Fig. 7. Binding of TRPC3 to calcineurin, Homer1 or FKBP12 is not affected by FKBP52 truncation mutants. (A) Co-IP of calcineurin (CaN) and TRPC3 in HEK 293 cells co-transfected with TRPC3, YFP–CaN together with HA–FKBP52 (aa 135–459) or an HA control plasmid. TRPC3 was bound to CaN in cells expressing TRPC3 and YFP–CaN (lane 2, top immunoblot) as well as in cells triple-transfected with TRPC3, YFP–CaN and HA–FKBP52 (aa 135–459; lane 3, top immunoblot). Representative immunoblots showing TRPC3 (top blot) co-immunoprecipitated with YFP–CaN (blot second from top). Expression of TRPC3, YFP–CaN and HA–FKBP52 (aa 135–459) was confirmed in the respective lysates. (B) Densitometric quantification of the TRPC3 protein fraction bound to CaN. Values were calculated relative to the lysate. Differences were not significant (P=0.86; one-way ANOVA with Holm–Sidak method), mean±s.e.m. (C) Co-IP of YFP–TRPC3 and endogenously expressed Homer1 and FKBP12 in HEK 293 cells. Binding of Homer1 to YFP–TRPC3 is not affected by the expression of HA–FKBP52 (aa 135–459) or HA-FKBP52 (aa 280–352). FKBP12 does not interact with YFP–TRPC3. The blots are representative of three independent experiments.

TRPC6 (Lopez et al., 2015; Sinkins et al., 2004). Regarding the regulation of TRPC1, it was shown that single point mutations in the PPIase domain of FKPB52 (FD67DV) and FKBP12 (D37L) failed to cause a considerable isomerization of N- and C-terminal structures in TRPC1 (Shim et al., 2009). Consequently, the spontaneous activity of TRPC1 was increased by the presence of the isomerase-dead FKBP12 mutation, and an agonist-induced TRPC1 activation was blocked when the catalase-impaired FKPB52 isoform was expressed (Shim et al., 2009). Based on our findings of the elevated TRPC3 current densities and Ca^{2+} signals that we elicited by expressing the FKBP52 truncation mutant FKBP52 (aa 280–352), we assume that the activity of TRPC3 is also regulated in an isomerase-dependent fashion, although, in contrast to other mammalian TRPC isoforms, towards an inhibitory functional state. Consequently, owing to an impaired interaction with FKBP52, TRPC3 might become more sensitive to stimulation and allow greater Ca^{2+} fluxes. As an additional mechanism in such situations, the *cis-trans* isomerization of TRPC3 through FKBP12 might contribute to an increased TRPC3 activation. FKBP12 was identified as a TRPC3 interaction partner in brain lysates, where it binds to the C-terminal PP motif in TRPC3 (Sinkins et al., 2004). A loss of interaction between TRPC3–FKBP52 might strengthen an association between FKBP12 and TRPC3, resulting in an increased channel activity during stimulation. Surprisingly, we could not detect endogenously expressed FKBP12 in TRPC3 immunoprecipitates, suggesting that the observed functional effects of FKBP52 in HEK 293 cells is unlikely to involve FKBP12. Our biochemical analyses also excluded the scaffold protein Homer1 as a regulator of the TRPC3–FKBP52 complex. Although TRPC3 associated with Homer1, the strength of interaction remained unchanged in the

Journal of Cell Science (2019) 132, jcs231506. doi:10.1242/jcs.231506

presence of FKBP52 structural fragments. Based on this experimental data, Homer1 does not seem to be recruited as part of a negative feedback mechanism that prevents an overactivation of TRPC3. However, future experiments with reduced Homer1 or FKBP12 levels are required to define the interplay with FKBP52 in HEK 293 cells as well as in native cardiomyocytes.

In cardiomyocytes, the physiological relevance of the FKBP52–TRPC3 coupling became apparent as an elevated agonist-dependent hypertrophic response. The rationale to analyze cardiomyocyte hypertrophy was based on the role of TRPC3 as a crucial mediator in the hypertrophic program translating GPCR stimuli to Ca^{2+}-dependent signaling proteins (Eder, 2017; Eder and Molkentin, 2011). The hypertrophic increase on the cellular level was achieved by an α-adrenergic- or Ang II-dependent stimulation of NRCs. Interestingly, the presence of Pyr3, a specific TRPC3 inhibitor (Kiyonaka et al., 2009), reduced the cardiomyocyte enlargement under conditions of FKBP52 knockdown. Based on these data, GPCR-dependent hypertrophic enlargement involves some degree of TRPC3 activity, which is further promoted when FKBP52 is downregulated. Importantly, Pyr3 also reduced the cell growth at baseline, pointing to a constitutive TRPC3 activity, a commonly described feature of this TRPC isoform (Dietrich et al., 2003). Following our hypothesis and in line with our functional data, the expression of structural FKBP52 domains lacking the PPIase site had similar effects, causing an increased cell enlargement with slightly upregulated ANP expression levels after GPCR stimulation, although without inducing a baseline hypertrophic response. This discrepancy compared to what was seen upon FKBP52 knockdown remains elusive. It could be based on an increased baseline activity of TRPC3, a tighter association with calcineurin or, speculatively, increased binding of FKBP12.6, which elevates the spontaneous TRPC3 activity as previously shown for TRPC1 in neurons (Shim et al., 2009).

Nevertheless, FKBP52 structural mutants were coupled with an enhanced baseline NFATc1 activation that was diminished by the TRPC3 inhibitor Pyr3. In addition, we observed an altered expressional profile of NFATc3 and HDAC4, which is characteristic of an increased hypertrophic enlargement during GPCR stimulation. Indeed, OAG and PE, as well as Ang II, induced a significant hypertrophic response in adult and neonatal cardiomyocytes when FKBP52 mutants were expressed. We assume that, during agonist activation, these structural FKBP52 mutants induce a TRPC3-mediated Ca^{2+} influx that evokes several signaling pathways, including those mediated by calcineurin/NFAT and the CamKII, that govern a pro-hypertrophic profile.

Interestingly, the treatment of cardiomyocytes with FK506 did not imitate the pro-hypertrophic phenotype of an FKBP52 knockdown by competing FKBP52 off from TRPC3. Since FK506 targets multiple intracellular receptors of the FKBP family, its potential role to displace FKBP52 from TRPC3 might be masked by other mechanisms. FK506 is best known for its inhibition of calcineurin through complex formation with FKBP12 (Li et al., 2011), which might be the dominating mechanism causing anti-hypertrophic effects in cardiomyocytes. Indeed, Gao et al. (2012) reported that FK506 blocked hypertrophy and calcineurin/NFAT activity in NRCs which, paradoxically, was induced by overexpressing TRPC3. These effects could very well be determined by a relief of stimulatory effects that are based on an FKBP12 *cis-trans* isomerization of TRPC3. In case of such a scenario, the use of FK506 as a calcineurin inhibitor (Wilkins and Molkentin, 2004) needs to be even more carefully evaluated. Referring to the functional relationship between FKBP52 and TRPC3, an inhibition of FKBP52 would most certainly cause adverse effects given its role in preventing calcineurin/NFAT activation and hypertrophy. The concept of this novel mechanism is worth investigating in the intact heart as part of future studies.

MATERIALS AND METHODS

Yeast two-hybrid growth screen

The Ras recruitment screen was performed as described previously (Aronheim, 2004; Kehat et al., 2011). In brief, the bait was a hybrid protein consisting of an activated Ras protein lacking its farnesylation CAAX box and the TRPC3 protein fragments [aa 1–341, 670–797 and 742–848 from the TRPC3 isoform 3 (UniProt Q13507-3)]. The bait plasmid was co-transfected into Cdc25-2 yeast cells with a myristoylated heart cDNA library (CryoTrap; Agilent Technologies). The expression of the cDNA library was under the control of the Gal1-inducible promoter, while the expression of the bait was controlled by a Met-off inducible promoter. Plates were incubated at the permissive temperature of 24°C for 7 days, were subsequently replicated onto inductive medium and incubated at the restrictive temperature of 36°C. Colonies with efficient growth were selected and grown on appropriate glucose plates for 2 days. Subsequently, galactose and methionine dependency were assayed by replica plating at the restrictive temperature of 36°C. Colonies that exhibited efficient cell growth and full dependency were further analyzed. The plasmid DNA was isolated, and the library plasmid identified by sequencing. Identified library plasmids were reintroduced into Cdc25-2 cells with the specific bait and the interaction was re-examined using the galactose and methionine dependency test at the restrictive temperature of 36°C.

Molecular biology, adenovirus generation and mRNA analysis

FKBP52 cDNA fragments encoding aa 1–138, 139–253, 230–303, 280–352, 352–459 and 135–459 were amplified by PCR using mouse FKBP52 as template and subcloned into pcDNA3.1 containing an HA sequence (a gift from Jeffery Molkentin, Cincinnati Children's Hospital Medical Center, OH). For the site-directed mutagenesis of the HA-cDNA fragment encoding FKBP52 (aa 352-459), the instructions of the QuikChange II Site-Directed Mutagenesis Kit from Agilent Technologies were followed. The following primer sequences were included in the PCR reaction: FW, 5′-GCCTGTTTCGCCGGGGAGAGGCCCA-3′; RV, 5′-TGGGCCTCT-CCCCGGCGAAACAGGC-3′. For the generation of adenoviruses, cDNAs encoding the FKBP52 protein fragments aa 280–352 or aa 135–459 were subcloned into pENTR 3C Dual Selection Vector and recombined with the pAd/CMV/V5-DEST™ vector following the Gateway® Technology (ThermoFisher Scientific).

Reverse transcription was performed using the SuperScript III First-Strand Synthesis System (Thermo Fisher Scientific). Analysis of *RCAN1* mRNA expression levels was performed using individual Taqman gene expression assays (Applied Biosystems). mRNA expression was quantified, normalized to GAPDH levels, and expressed relative to levels in βgal-infected cells.

HEK 293 culture and transfection

HEK 293 cells were obtained from ATCC (CRL-1573). The stable TRPC3 cell line T3.9 was provided in a collaboration with the Medical University of Graz, Austria (Poteser et al., 2006). The cell lines were regularly tested to confirm the absence of mycoplasma (Applichem). The cells were cultured in Dulbecco's modified Eagle's medium with high glucose (DMEM; Sigma-Aldrich) supplemented with 10% fetal bovine serum (FBS; Sigma-Aldrich), 100 U/ml penicillin, 100 µg/ml streptomycin (PAN Biotech) at 37°C and 5% CO_2. T3.9 cells were additionally treated with the antibiotics G418 (0.5 mg/ml; Sigma-Aldrich). HEK 293 cells were transiently co-transfected with HA-tagged FKBP52 protein fragments, human TRPC3-pcDNA3 (a gift from Jeffery Molkentin, Cincinnati Children's Hospital Medical Center, USA), YFP–TRPC3 (human) (a gift from Klaus Groschner, Medical University of Graz, Austria; Lichtenegger et al., 2013), full-length (mouse) FKBP52-pCMV SPORT6 (Open Biosystems) and/or EGFP–calcineurin (human) (Olivares-Florez et al., 2018) using the X-tremeGENE HP DNA Transfection Reagent (Roche) (1:1 ratio of reagent to DNA).

Journal of Cell Science (2019) 132, jcs231506. doi:10.1242/jcs.231506

Neonatal and adult rat cardiomyocyte cultures, adenoviral infections and siRNA treatment

All animal experiments were approved by the authority of Unterfranken and the standing authority of the University Hospital of Würzburg (permit number, 55-2-2531.01-77/13). NRCs were isolated from 1–3-day-old Wistar rats (Charles River Laboratories). After the decapitation, the hearts were quickly removed and rinsed with ice-cold Ca^{2+} and bicarbonate-free Hanks Hepes buffer (in mmol/l: NaCl 137, KCl 5.366, $MgSO_4{\times}7H_2O$ 0.811, Dextrose 5.55, KH_2PO_4 0.44, Na_2HPO_4 0.34, Hepes 20.06; pH 7.4). The subsequent steps of isolation were as described previously (Kirschmer et al., 2016) with some variations. The isolated cardiomyocytes were cultured in minimal essential medium (MEM) with 5% FBS (MEM/5% FBS). After 24 h, the cells were washed with PBS and cultured for additional 24 h in MEM/5% FBS. The cells were infected with adenoviruses encoding βgal, N-terminally mouse HA-tagged FKBP52 (aa 280–352 or aa 135–459), human NFATc1–GFP or mouse TRPC6 (from Seven Hills Bioreagents Cincinnati, USA). The titer was determined by using the Quick Titer Adenovirus Titer ELISA Kit (CELL BIOLABS) and the plaque assay (Baer and Kehn-Hall, 2014). The adenoviruses were applied at a multiplicity of infection (MOI) of 50–100 and applied in OptiMEM for 4 h and kept in MEM/1% FBS for further 24 h. For the evaluation of agonist-induced hypertrophy, cells were serum-starved for 24 h and stimulated with Ang II (100 nM; Sigma-Aldrich), PE (50 µM; Sigma-Aldrich), OAG (100 µM) or vehicle for 24 h. In some experiments, FK506 (2 µM; Sigma-Aldrich) was added to the cells. To analyze the nuclear translocation of NFATc1, cells were pre-treated with Pyr3 (10 µM; Calbiochem) or vehicle for 6 h and stimulated with Ang II (1 µM), PE (50 µM) or vehicle for 15 min.

To downregulate endogenous FKBP52 in NRCs and T3.9 cells, the ON-TARGETplus SMARTpool FKBP4 (FKBP52) siRNA from Dharmacon was used and transfected using Lipofectamine RNAiMAX (Life Technologies) according to the manufacturer's instructions. As a control, we used the ON-TARGETplus Non-targeting Pool. After 48 h, cells were stimulated with PE (50 µM), Pyr3 (10 µM) or vehicle for 24 h followed by immunocytochemistry or western blotting.

Adult rat cardiomyocytes were isolated from 5-month-old female Wister rats (Charles River Laboratories). The rats were anesthetized with 5% isoflurane in O_2 and a mixture of buprenorphine (0.05 mg/kg body weight) and heparin (500 IU/kg body weight). After opening the thorax, the heart was removed and cannulated through the aorta on a Langendorff apparatus to perform a retrograde perfusion with a buffer (in mmol/l: NaCl, 113.01; KCl, 4.69; KH_2PO_4, 0.6; Na_2HPO_4, 0.6; $MgSO_4{\cdot}7H_2O$; 1.22; Phenol Red, 0.032; $NaHCO_3$, 12.02; $KHCO_3$, 10; HEPES buffer solution, 10; glucose, 5.5; taurine, 30; and 2,3-butanedione monoxime (BDM), 10). After 4 min, the perfusion buffer was switched to a digestion buffer containing 0.072 mg/ml Liberase TH (Roche). The enzymatic digestion was continued until the heart became swollen and slightly pale (6–10 min). The atria were removed, and the remaining ventricles were put in a dish containing 5 ml of perfusion buffer. After cutting the tissue, 5 ml stopping buffer (perfusion buffer with 10% FCS and 12.5 µM $CaCl_2$) was added for 5 min until the cells settled down. The supernatant was discarded and the cell pellet resuspended in 10 ml stopping buffer 2 (perfusion buffer with 5% FCS and 12.5 µM $CaCl_2$) to start the Ca^{2+} reintroduction ($CaCl_2$ solution: 50 µl 10 mM, 50 µl 10 mM, 100 µl 10 mM, 30 µl 100 mM, 50 µl 100 mM). After the last step, the cells were resuspended in plating medium (Medium199; Sigma-Aldrich) supplemented with 5% fetal bovine serum (FBS), 50 U/ml penicillin, 50 µg/ml streptomycin (PAN Biotech), 870 nM insulin, 65 nM transferrin, 29 nM Na-selenite, 0.1% BDM (all reagents Sigma-Aldrich unless otherwise indicated). The isolated cells were cultured for 3 h and infected with adenoviruses encoding βgal or N-terminally HA-tagged FKBP52 (aa 135–459). The adenoviruses were applied in a MOI of 50–100 in culture medium (Medium199) supplemented with 50 U/ml penicillin, 50 µg/ml streptomycin (PAN Biotech), 870 nM insulin, 65 nM transferrin, 29 nM Na-selenite and 25 µM (-)-blebbistatin (all reagents Sigma-Aldrich unless otherwise indicated) for 24 h. The cells were then stimulated with PE (50 µM) or vehicle in culture medium for 24 h.

Immunocytochemistry, cell surface measurements and NFAT translocation

NRCs or adult rat cardiomyocytes were cultured on laminin (BD Sciences)-coated coverslips. After adenoviral infection or siRNA transfection, serum starvation and stimulation with Ang II or PE, cells were fixed with 4% paraformaldehyde, washed with PBS, permeabilized with 0.5% Triton X-100 and blocked with a solution containing 1% BSA, 0.1% cold water fish skin gelatin and 1% Tween-20, as described previously (Kirschmer et al., 2016). Cells were then labeled using an antibody against α-actinin (1:200; cat. no A7811, Sigma-Aldrich) and a secondary antibody (Alexa Fluor 568, 1:400; Life Technologies) to visualize cardiomyocytes, as well as DAPI to visualize the nucleus (300 nM; Life Technologies). Fluorescence microscopy was performed by using a Zeiss Axiovert 135 microscope (Zeiss Plan Neofluar) or a Leica DMi8 microscope (Leica Microsystems). The NRC size was determined at least in duplicate cell culture dishes of at least three different cardiomyocyte isolations. The cell size of at least 50 cells/cell culture dish was analyzed by using Image J or the LASX software (Leica). Quantification of the nuclear translocation of NFATc1 was determined by measuring the mean gray value of NFATc1–GFP in the nucleus and in the cytoplasm and calculating the quotient of the values. At least 50 cells/cell culture dish in duplicate cell culture dishes of at least three different cardiomyocyte isolations were analyzed by using the LAS X software (Leica). The size of adult rat cardiomyocytes was determined by light microscopy.

Isolation of protein fractions from NRCs

NRCs were treated as described in Fassett et al. (2009). They were washed once with PBS pH 7.4 at room temperature (RT), treated with lysis buffer [containing 1% Triton X-100, 1 mM EDTA, 100 mM NaCl, 1× protease inhibitor cocktail (Roche) and phosphatase inhibitor cocktail set II (Merck Millipore) and phosphatase inhibitor cocktail set IV (Merck Millipore), and 10% glycerol, in 10 mM Tris HCl pH 7.4]. Following this procedure, cytosolic and membrane proteins were released. Intact cytoskeleton, adhesion proteins and insoluble nuclear material remained attached to the plate and was collected in 2× SDS loading buffer (4% SDS, 20% glycerol, in 125 mM Tris-HCl pH 6.8) and used for western blotting.

Co-immunoprecipitation and western blotting

Protein lysates from HEK 293 cells and adult mouse hearts (wild type; FVB/N) were prepared in a buffer containing 50 mM Tris-HCl pH 7.4, 150 mM NaCl, 1% Triton X-100, 0.5 mM DTT and a protease inhibitor cocktail (Roche) as described previously (Kirschmer et al., 2016; Wu et al., 2010). After a step of preclearing with appropriate control IgGs, the lysates were treated with the following antibodies: anti-HA (Santa Cruz Biotechnology, #sc-7392), anti-GFP (Abcam, #ab290) or anti-FKBP52 (Santa Cruz Biotechnology, #sc-1803) antibodies. Western blotting of protein extracts from HEK 293 cells, NRCs and mouse hearts was performed with the following antibodies: anti-FKBP52 (Santa Cruz Biotechnology, #sc-1803), anti-HA (Santa Cruz Biotechnology, #sc-7392), anti-HA (Cell Signaling Technology, #3724), anti-GFP (Abcam, #ab290), anti-TRPC3 (custom-made; Poteser et al., 2006), anti-GAPDH (Millipore, #MAB374), anti-Homer1 (Abcam, #ab211415), anti-FKBP12 (Thermo Fisher Scientific, #PA1-026A), anti-detyrosinated-tubulin (Merck Millipore, #AB3201), anti-α-Tubulin (Cell Signaling Technology, #2144) or anti-Lamin A/C (Cell Signaling Technology, #2032) antibodies followed by horseradish peroxidase-conjugated antibodies [ECL horseradish peroxidase labeled anti-rabbit-IgG antibody, (GE Healthcare, #NA934) or ECL anti-mouse-IgG horseradish peroxidase linked whole antibody (GE Healthcare, #NA931)]. All primary antibodies were diluted 1:1000 and the secondary antibodies at 1:3000. All immunoblots were analyzed by using a chemiluminescence detection system (Biorad).

Cytosolic Ca^{2+} measurements

HEK 293 cells, T3.9 cells or NRCs were cultured on coverslips and loaded with Fura 2-AM (2 µM; Thermo Fisher Scientific) and probenecid (0.5 mM; Thermo Fisher Scientific) in a nominally Ca^{2+}-free normal Tyrode (NT) solution (mmol/l: NaCl, 140; KCl, 4; $MgCl_2$, 1; Hepes, 5; glucose, 10; pH 7.4) for 40 min at RT. HEK 293 cells and NRCs were stimulated with OAG (100 µM; Sigma-Aldrich) and T3.9 cells were stimulated with carbachol (300 µM; Sigma-Aldrich) in nominally Ca^{2+}-free conditions, and perfused with 2 mM extracellular $CaCl_2$. Cytosolic Ca^{2+} levels were calculated as the fluorescence ratio of that at 340 nm and to that at 380 nm (denoted

F340/380). Measurements were performed by using the 'Myocyte and Contractility System' from Ionoptix and data were analyzed by using the IonWizard 6.3 software (Ionoptix). Transfected cells from at least three different cultures were included in the analysis.

Electrophysiology

Whole-cell voltage-clamp experiments in HEK 293 cells were performed using an L/A-EPC7-Amplifier (List Medical Electronic) and a Digidata-1322A Digitizer (Axon Instruments) as previously described (Lichtenegger et al., 2013). Standard extracellular and intracellular solutions were used as described previously (Lichtenegger et al., 2013). Linear voltage-ramps were applied ranging from −130 to +80 mV. Current values were taken at −90 mV (inward) and at +70 mV (outward) and normalized to the cell capacitance.

Statistical analysis

Means±s.e.m. are presented for all data analyses. The two-tailed unpaired Student's *t*-test was used to analyze significant differences between two groups. Significant differences between more than two groups were assessed by one-way ANOVA with the Holm–Sidak method. Two-way ANOVA followed by the Holm–Sidak method was used to detect significant differences when variables were dependent on two factors. In Figs 3B, 4B and Fig. S2, the two-way ANOVA with Holm–Sidak method was used to compare data within the control and stimulatory group, respectively, and the two-tailed unpaired Student's *t*-test between data of the control and treatment groups. In Fig. 2, the Analysis of Variance on Ranks followed by the Dunn's method was applied to detect significant differences between the groups. All analyses were performed by using SigmaPlot 13. $P \leq 0.05$ was considered significant.

Acknowledgements

We thank Alice Schaaf, Anna-Karina Lamprecht, Michelle Gulentz, Annette Berbner and Katharina Marnet for their excellent technical assistance. We also thank Dr Michael Kohlhaas for supporting electrophysiological recordings.

Competing interests

The authors declare no competing or financial interests.

Author contributions

Conceptualization: P.E.-N.; Methodology: S.B., P.P.S., S.P., O.T., A.C., E.M.-L.; Validation: P.E.-N.; Formal analysis: S.B., O.T.; Investigation: S.B., P.P.S., S.P., O.T., A.C.; Writing - original draft: P.E.-N.; Writing - review & editing: E.M.-L.; Supervision: P.E.-N.; Project administration: P.E.-N.; Funding acquisition: P.E.-N.

Funding

This work was supported by grants from the Bundesministerium für Bildung und Forschung (BMBF01 EO1004 and 01EO1505) through the Comprehensive Heart Failure Center and the Deutsche Forschungsgemeinschaft (ED 266/1-1, MI 2114/1-1).

Supplementary information

Supplementary information available online at
http://jcs.biologists.org/lookup/doi/10.1242/jcs.231506.supplemental

References

Aronheim, A. (2004). Ras signaling pathway for analysis of protein-protein interactions in yeast and mammalian cells. *Methods Mol. Biol.* **250**, 251-262. doi:10.1385/1-59259-671-1:251

Backs, J., Song, K., Bezprozvannaya, S., Chang, S. and Olson, E. N. (2006). CaM kinase II selectively signals to histone deacetylase 4 during cardiomyocyte hypertrophy. *J. Clin. Invest.* **116**, 1853-1864. doi:10.1172/JCI27438

Baer, A. and Kehn-Hall, K. (2014). Viral concentration determination through plaque assays: using traditional and novel overlay systems. *J. Vis. Exp.*, **93**, e52065. doi:10.3791/52065

Bonner, J. M. and Boulianne, G. L. (2017). Diverse structures, functions and uses of FK506 binding proteins. *Cell. Signal.* **38**, 97-105. doi:10.1016/j.cellsig.2017.06.013

Chambraud, B., Belabes, H., Fontaine-Lenoir, V., Fellous, A. and Baulieu, E. E. (2007). The immunophilin FKBP52 specifically binds to tubulin and prevents microtubule formation. *FASEB J.* **21**, 2787-2797. doi:10.1096/fj.06-7667com

Cheung-Flynn, J., Roberts, P. J., Riggs, D. L. and Smith, D. F. (2003). C-terminal sequences outside the tetratricopeptide repeat domain of FKBP51 and FKBP52 cause differential binding to Hsp90. *J. Biol. Chem.* **278**, 17388-17394. doi:10.1074/jbc.M300955200

Dietrich, A., Mederos y Schnitzler, M., Emmel, J., Kalwa, H., Hofmann, T. and Gudermann, T. (2003). N-linked protein glycosylation is a major determinant for basal TRPC3 and TRPC6 channel activity. *J. Biol. Chem.* **278**, 47842-47852. doi:10.1074/jbc.M302983200

Dietrich, A., Kalwa, H., Rost, B. R. and Gudermann, T. (2005). The diacylglycerol-sensitive TRPC3/6/7 subfamily of cation channels: functional characterization and physiological relevance. *Pflugers Arch.* **451**, 72-80. doi:10.1007/s00424-005-1460-0

Eder, P. (2017). Cardiac remodeling and disease: SOCE and TRPC signaling in cardiac pathology. *Adv. Exp. Med. Biol.* **993**, 505-521. doi:10.1007/978-3-319-57732-6_25

Eder, P. and Molkentin, J. D. (2011). TRPC channels as effectors of cardiac hypertrophy. *Circ. Res.* **108**, 265-272. doi:10.1161/CIRCRESAHA.110.225888

Eder, P., Schindl, R., Romanin, C. and Groschner, K. (2007). Protein–protein interactions in TRPC channel complexes. In *TRP Ion Channel Function in Sensory Transduction and Cellular Signaling Cascades* (ed. W. B. Liedtke and S. Heller). pp. 331-348. Boca Raton, FL: CRC Press/Taylor & Francis.

Erlejman, A. G., Lagadari, M., Harris, D. C., Cox, M. B. and Galigniana, M. D. (2014). Molecular chaperone activity and biological regulatory actions of the TPR-domain immunophilins FKBP51 and FKBP52. *Curr. Protein Pept. Sci.* **15**, 205-215. doi:10.2174/1389203715666140331113753

Fan, C., Choi, W., Sun, W., Du, J. and Lu, W. (2018). Structure of the human lipid-gated cation channel TRPC3. *eLife* **7**, e36852. doi:10.7554/eLife.36852

Fassett, J. T., Xu, X., Hu, X., Zhu, G., French, J., Chen, Y. and Bache, R. J. (2009). Adenosine regulation of microtubule dynamics in cardiac hypertrophy. *Am. J. Physiol. Heart Circ. Physiol.* **297**, H523-H532. doi:10.1152/ajpheart.00462.2009

Freichel, M., Berlin, M., Schürger, A., Mathar, I., Bacmeister, L., Medert, R., Frede, W., Marx, A., Segin, S. and Londoño, J. E. C. (2017). TRP channels in the heart. In *Neurobiology of TRP Channels* (ed. T. L. R. Emir). pp. 149-185. Boca Raton, FL: CRC Press/Taylor & Francis.

Gaburjakova, M., Gaburjakova, J., Reiken, S., Huang, F., Marx, S. O., Rosemblit, N. and Marks, A. R. (2001). FKBP12 binding modulates ryanodine receptor channel gating. *J. Biol. Chem.* **276**, 16931-16935. doi:10.1074/jbc.M100856200

Gao, H., Wang, F., Wang, W., Makarewich, C. A., Zhang, H., Kubo, H., Berretta, R. M., Barr, L. A., Molkentin, J. D. and Houser, S. R. (2012). Ca(2+) influx through L-type Ca(2+) channels and transient receptor potential channels activates pathological hypertrophy signaling. *J. Mol. Cell. Cardiol.* **53**, 657-667. doi:10.1016/j.yjmcc.2012.08.005

Goel, M., Garcia, R., Estacion, M. and Schilling, W. P. (2001). Regulation of Drosophila TRPL channels by immunophilin FKBP59. *J. Biol. Chem.* **276**, 38762-38773. doi:10.1074/jbc.M104125200

He, X., Li, S., Liu, B., Susperreguy, S., Formoso, K., Yao, J., Kang, J., Shi, A., Birnbaumer, L. and Liao, Y. (2017). Major contribution of the 3/6/7 class of TRPC channels to myocardial ischemia/reperfusion and cellular hypoxia/reoxygenation injuries. *Proc. Natl. Acad. Sci. USA* **114**, E4582-E4591. doi:10.1073/pnas.1621384114

Ivery, M. T. G. (2000). Immunophilins: switched on protein binding domains? *Med. Res. Rev.* **20**, 452-484. doi:10.1002/1098-1128(200011)20:6<452::AID-MED2>3.0.CO;2-6

Kehat, I., Accornero, F., Aronow, B. J. and Molkentin, J. D. (2011). Modulation of chromatin position and gene expression by HDAC4 interaction with nucleoporins. *J. Cell Biol.* **193**, 21-29. doi:10.1083/jcb.201101046

Kirschmer, N., Bandleon, S., von Ehrlich-Treuenstätt, V., Hartmann, S., Schaaf, A., Lamprecht, A.-K., Miranda-Laferte, E., Langsenlehner, T., Ritter, O. and Eder, P. (2016). TRPC4α and TRPC4β similarly affect neonatal cardiomyocyte survival during chronic GPCR stimulation. *PLoS ONE* **11**, e0168446. doi:10.1371/journal.pone.0168446

Kiyonaka, S., Kato, K., Nishida, M., Mio, K., Numaga, T., Sawaguchi, Y., Yoshida, T., Wakamori, M., Mori, E., Numata, T. et al. (2009). Selective and direct inhibition of TRPC3 channels underlies biological activities of a pyrazole compound. *Proc. Natl. Acad. Sci. USA* **106**, 5400-5405. doi:10.1073/pnas.0808793106

Kuwahara, K., Wang, Y., McAnally, J., Richardson, J. A., Bassel-Duby, R., Hill, J. A. and Olson, E. N. (2006). TRPC6 fulfills a calcineurin signaling circuit during pathologic cardiac remodeling. *J. Clin. Invest.* **116**, 3114-3126. doi:10.1172/JCI27702

Lehnart, S. E., Huang, F., Marx, S. O. and Marks, A. R. (2003). Immunophilins and coupled gating of ryanodine receptors. *Curr. Top. Med. Chem.* **3**, 1383-1391. doi:10.2174/1568026033451907

Li, H., Rao, A. and Hogan, P. G. (2011). Interaction of calcineurin with substrates and targeting proteins. *Trends Cell Biol.* **21**, 91-103. doi:10.1016/j.tcb.2010.09.011

Lichtenegger, M., Stockner, T., Poteser, M., Schleifer, H., Platzer, D., Romanin, C. and Groschner, K. (2013). A novel homology model of TRPC3 reveals allosteric coupling between gate and selectivity filter. *Cell Calcium* **54**, 175-185. doi:10.1016/j.ceca.2013.05.010

Lopez, E., Berna-Erro, A., Salido, G. M., Rosado, J. A. and Redondo, P. C. (2015). FKBP25 and FKBP38 regulate non-capacitative calcium entry through TRPC6. *Biochim. Biophys. Acta* **1853**, 2684-2696. doi:10.1016/j.bbamcr.2015.07.023

Martínez-Martínez, S. and Redondo, J. M. (2004). Inhibitors of the calcineurin/NFAT pathway. *Curr. Med. Chem.* **11**, 997-1007. doi:10.2174/0929867043455576

Nakayama, H., Wilkin, B. J., Bodi, I. and Molkentin, J. D. (2006). Calcineurin-dependent cardiomyopathy is activated by TRPC in the adult mouse heart. *FASEB J.* **20**, 1660-1670. doi:10.1096/fj.05-5560com

Olivares-Florez, S., Czolbe, M., Riediger, F., Seidlmayer, L., Williams, T., Nordbeck, P., Strasen, J., Glocker, C., Jänsch, M., Eder-Negrin, P. et al. (2018). Nuclear calcineurin is a sensor for detecting Ca2+ release from the nuclear envelope via IP3R. *J. Mol. Med.* **96**, 1239-1249. doi:10.1007/s00109-018-1701-2

Poteser, M., Graziani, A., Rosker, C., Eder, P., Derler, I., Kahr, H., Zhu, M. X., Romanin, C. and Groschner, K. (2006). TRPC3 and TRPC4 associate to form a redox-sensitive cation channel. Evidence for expression of native TRPC3-TRPC4 heteromeric channels in endothelial cells. *J. Biol. Chem.* **281**, 13588-13595. doi:10.1074/jbc.M512205200

Ramsey, I. S., Delling, M. and Clapham, D. E. (2006). An introduction to TRP channels. *Annu. Rev. Physiol.* **68**, 619-647. doi:10.1146/annurev.physiol.68.040204.100431

Rinne, A., Kapur, N., Molkentin, J. D., Pogwizd, S. M., Bers, D. M., Banach, K. and Blatter, L. A. (2010). Isoform- and tissue-specific regulation of the Ca(2+)-sensitive transcription factor NFAT in cardiac myocytes and heart failure. *Am. J. Physiol. Heart Circ. Physiol.* **298**, H2001-H2009. doi:10.1152/ajpheart.01072.2009

Shim, S., Yuan, J. P., Kim, J. Y., Zeng, W., Huang, G., Milshteyn, A., Kern, D., Muallem, S., Ming, G. and Worley, P. F. (2009). Peptidyl-prolyl isomerase FKBP52 controls chemotropic guidance of neuronal growth cones via regulation of TRPC1 channel opening. *Neuron* **64**, 471-483. doi:10.1016/j.neuron.2009.09.025

Sinkins, W. G., Goel, M., Estacion, M. and Schilling, W. P. (2004). Association of immunophilins with mammalian TRPC channels. *J. Biol. Chem.* **279**, 34521-34529. doi:10.1074/jbc.M401156200

Sivils, J. C., Storer, C. L., Galigniana, M. D. and Cox, M. B. (2011). Regulation of steroid hormone receptor function by the 52-kDa FK506-binding protein (FKBP52). *Curr. Opin. Pharmacol.* **11**, 314-319. doi:10.1016/j.coph.2011.03.010

Strübing, C., Krapivinsky, G., Krapivinsky, L. and Clapham, D. E. (2003). Formation of novel TRPC channels by complex subunit interactions in embryonic brain. *J. Biol. Chem.* **278**, 39014-39019. doi:10.1074/jbc.M306705200

Tiapko, O. and Groschner, K. (2018). TRPC3 as a target of novel therapeutic interventions. *Cells* **7**, 83. doi:10.3390/cells7070083

Trebak, M., Hempel, N., Wedel, B. J., Smyth, J. T., Bird, G. S. J. and Putney, J. W. (2005). Negative regulation of TRPC3 channels by protein kinase C-mediated phosphorylation of serine 712. *Mol. Pharmacol.* **67**, 558-563. doi:10.1124/mol.104.007252

Vazquez, G., Wedel, B. J., Aziz, O., Trebak, M. and Putney, J. W. (2004). The mammalian TRPC cation channels. *Biochim. Biophys. Acta* **1742**, 21-36. doi:10.1016/j.bbamcr.2004.08.015

Wilkins, B. J. and Molkentin, J. D. (2004). Calcium-calcineurin signaling in the regulation of cardiac hypertrophy. *Biochem. Biophys. Res. Commun.* **322**, 1178-1191. doi:10.1016/j.bbrc.2004.07.121

Wu, X., Eder, P., Chang, B. and Molkentin, J. D. (2010). TRPC channels are necessary mediators of pathologic cardiac hypertrophy. *Proc. Natl. Acad. Sci. USA* **107**, 7000-7005. doi:10.1073/pnas.1001825107

Yuan, J. P., Kiselyov, K., Shin, D. M., Chen, J., Shcheynikov, N., Kang, S. H., Dehoff, M. H., Schwarz, M. K., Seeburg, P. H., Muallem, S. et al. (2003). Homer binds TRPC family channels and is required for gating of TRPC1 by IP3 receptors. *Cell* **114**, 777-789. doi:10.1016/S0092-8674(03)00716-5

Zhang, Y., Knight, W., Chen, S., Mohan, A. and Yan, C. (2018). Multiprotein complex with TRPC (Transient Receptor Potential-Canonical) channel, PDE1C (Phosphodiesterase 1C), and A2R (Adenosine A2 Receptor) plays a critical role in regulating cardiomyocyte cAMP and survival. *Circulation* **138**, 1988-2002. doi:10.1161/CIRCULATIONAHA.118.034189

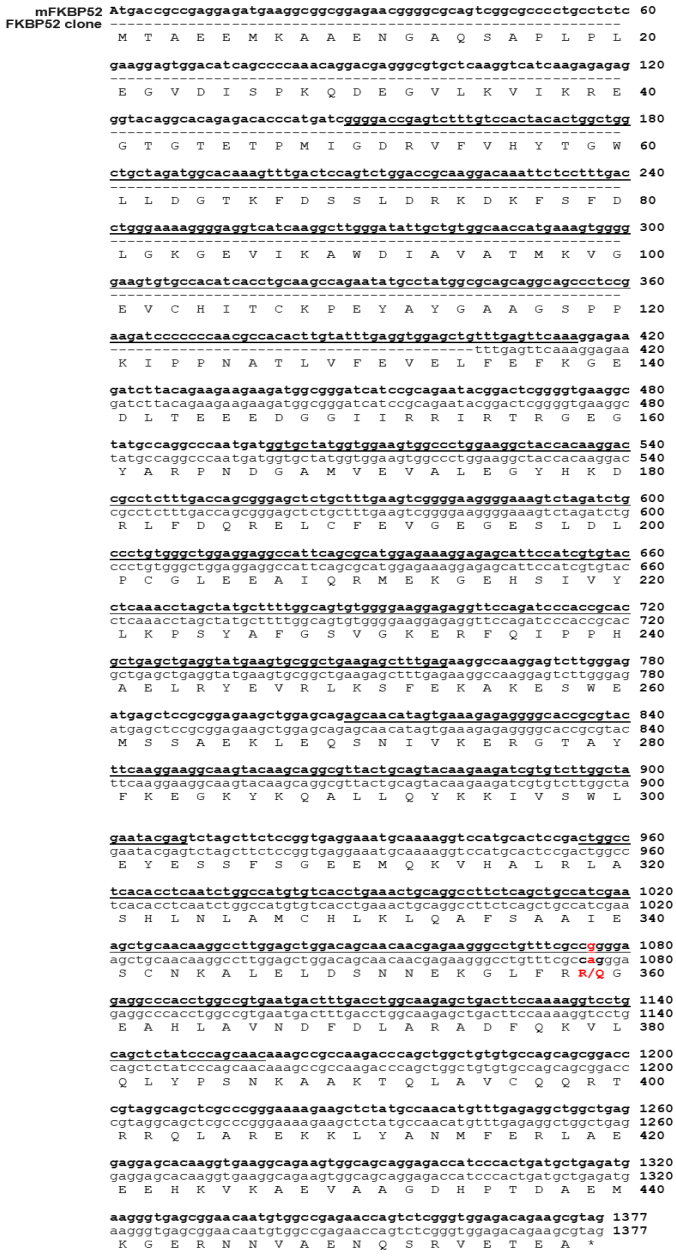

Fig. S1. **Sequence alignment of mouse FKBP52 (mFKBP52) and the FKBP52 cDNA clone from the screen.** Underlined sequences represent FKBP52 domains. The point mutation G1075A in the FKBP52 clone is marked in red.

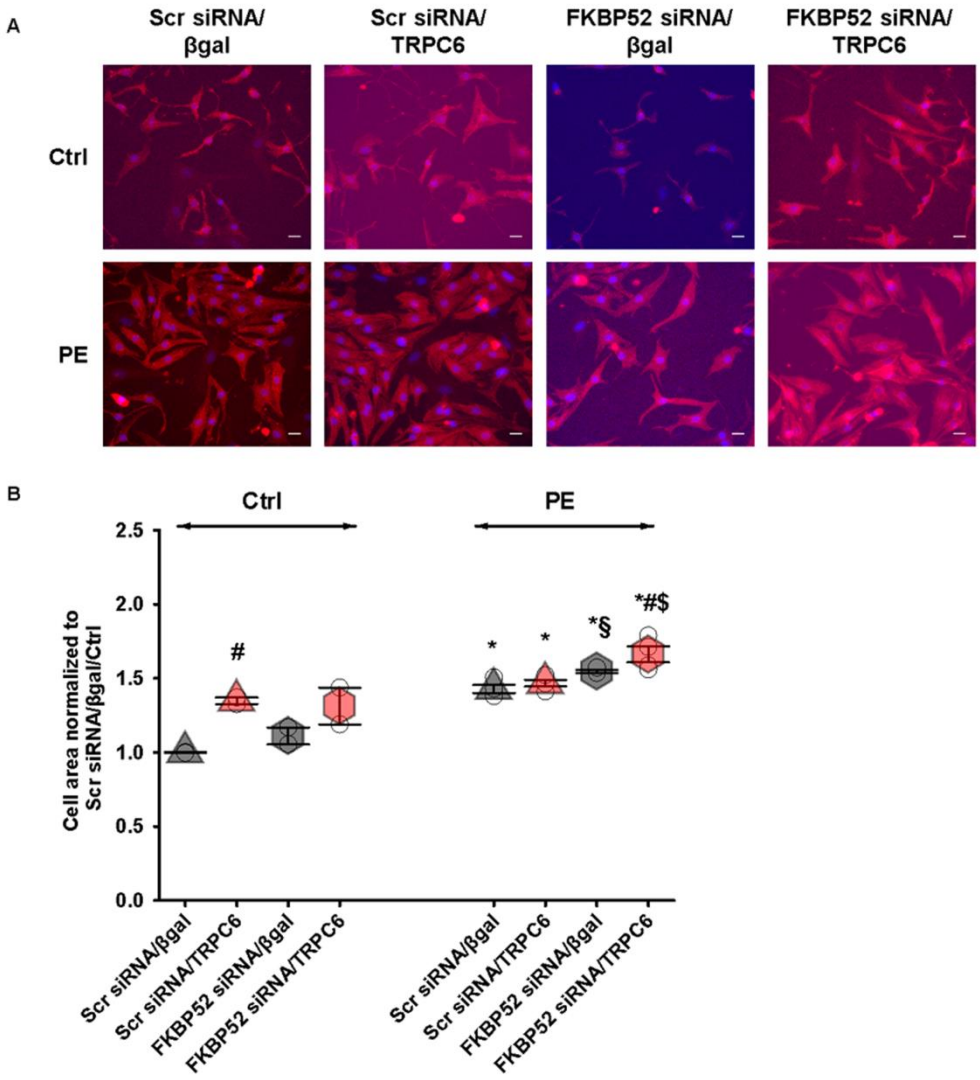

Fig. S2. Downregulation of FKBP52 results in an elevated TRPC6-induced hypertrophic response. (A) Neonatal rat cardiomyocytes (NRCs) were infected with adenoviruses encoding βgal or TRPC6 and transfected with FKBP52 (FKBP52 siRNA) or scramble siRNAs (Scr siRNA). The hypertrophic growth of NRCs was measured as an increase of the cell surface after phenylephrine (PE; 50 µM) or control (Ctrl) stimulation for 24 h. Red, α-actinin; Blue, DAPI. Scale bar: 20 µm. Taken with a 40× magnification objective. (B) Quantification of the cell area relative to Scr siRNA/βgal/Ctrl. *P<0.05 vs. respective Ctrl stimulation, $^{\#}$P<0.05 vs. Scr siRNA/βgal/Ctrl or vs. FKBP52 siRNA/βgal/PE, respectively, §P<0.05 vs. Scr siRNA/ βgal/PE, $^{\$}$P<0.05 vs. FKBP52 siRNA/ βgal/PE (two-way Anova with Holm-Sidak method and unpaired t-test), *n* = 2-4, mean ± SEM.

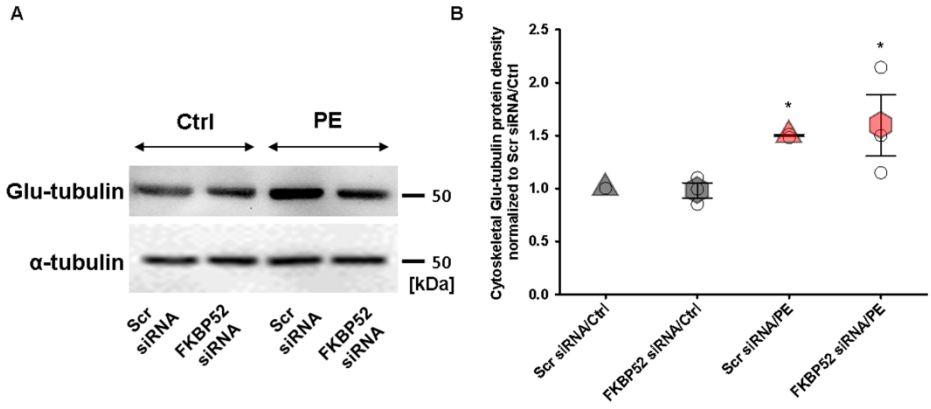

Fig S3. The stabilization of microtubules is not affected by a downregulation of FKBP52 during hypertrophic stimulation. (A) Western blot analysis of α-tubulin and Glu-tubulin expression levels in cytoskeletal extracts from neonatal rat cardiomyocytes (NRCs) after 24 h of phenylephrine (PE) or control (Ctrl) stimulation. The cells were transfected with FKBP52 or scramble siRNAs (Scr siRNA). (B) PE stimulation results in increased Glu-tubulin expression levels in FKBP52 and scr siRNA-treated NRCs. Protein expression levels were normalized to scr siRNA/Ctrl. *P<0.05 vs. to scr siRNA/Ctrl or FKBP52 siRNA /Ctrl, respectively (two-way Anova with Holm-Sidak method), *n* = 3, mean ± SEM.

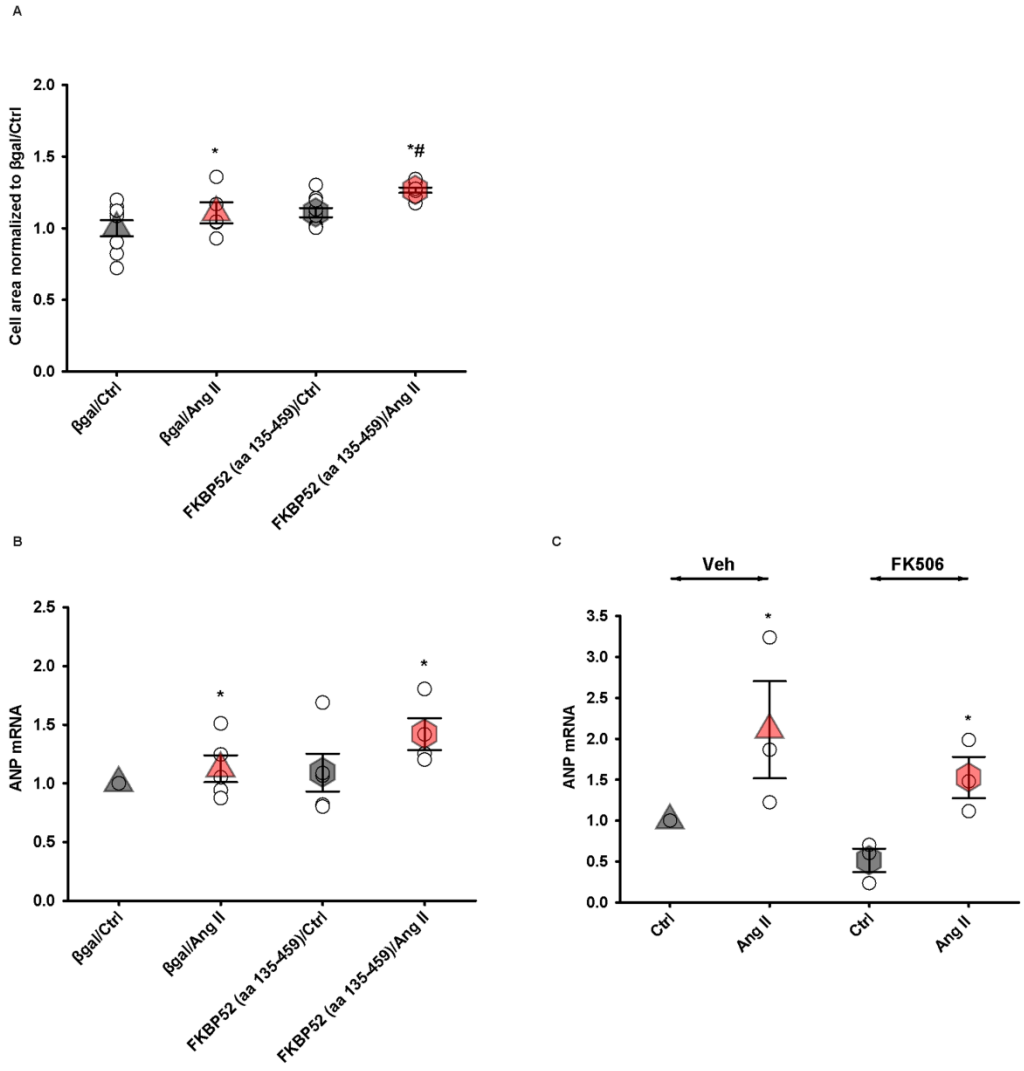

Fig S4. FKBP52 (aa 135-459) affects an angiotensin II-stimulated hypertrophic response differently than FK506. (A) Quantification of the cell area after 24 h of angiotensin II (Ang II; 100 nM) or control (Ctrl) stimulation. NRCs were infected with FKBP52 (aa 135-459) or βgal. Data are shown relative to βgal-infected controls. *P<0.05 vs. βgal/Ctrl, #P<0.05 vs. βgal/Ang II (two-way Anova with Holm-Sidak method), *n* = 5-9, mean ± SEM. (B) mRNA levels of atrial natriuretic peptide (ANP) were determined after 24 h of Ang II or control (Ctrl) stimulation *via* qPCR from NRCs expressing βgal or FKBP52 (aa 135-459). *P<0.05 vs. βgal or FKBP52 (aa 135-459)/Ctrl (two-way Anova with Holm-Sidak method), *n* = 4-5, mean ± SEM. (C) mRNA levels from NRCs treated with FK506 (2 µM) or vehicle (Veh). *P<0.05 vs. Ctrl (two-way Anova with Holm-Sidak method), *n* = 3, mean ± SEM. *P<0.05.

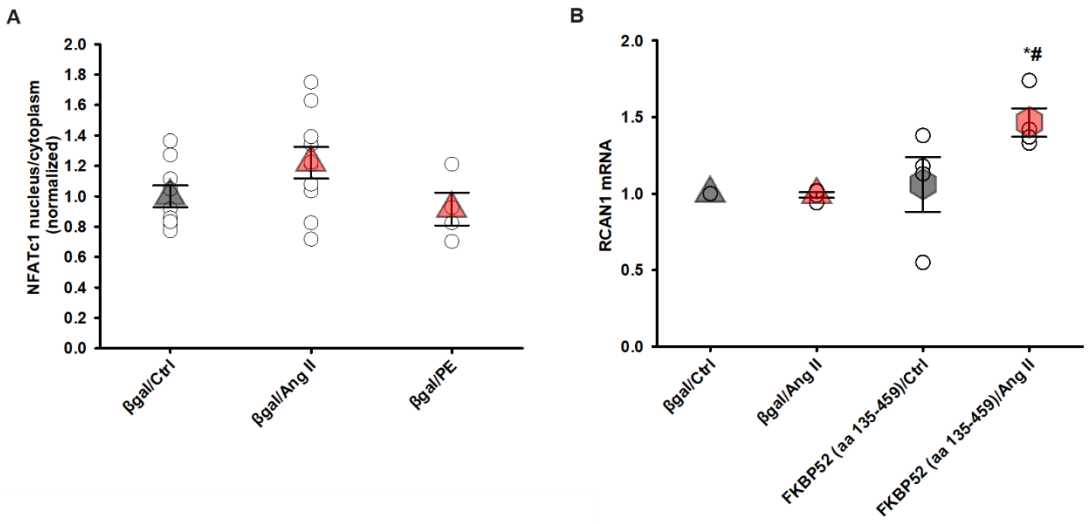

Fig. S5. NFATc1 and RCAN1 activation in response to agonist stimulation in neonatal rat cardiomyocytes. (A) Average quantified values of NFATc1-GFP localized to the nucleus in response to angiotensin II (Ang II; 100 nM), phenylephrine (PE; 50 µM) or control (Ctrl) stimulation. Neonatal rat cardiomyocytes (NRCs) were infected with βgal. Data are shown relative to βgal/Ctrl (One-way Anova with Holm-Sidak method), *n* = 4-10, mean ± SEM. (B) Regulator of calcineurin 1 (RCAN1) expression levels as parameter of the activation of calcineurin in NRCs. mRNA levels of RCAN1 were measured after 24 h of Ang II or control (Ctrl) stimulation *via* qPCR. NRCs were infected with βgal or FKBP52 (aa 135-459). Average quantified values relative to βgal/Ctrl. *P<0.05 vs. FKBP52 (aa 135-459)/Ctrl, $^{\#}$P<0.05 vs. βgal/ Ang II (two-way Anova with Holm-Sidak method), *n* = 4, mean ± SEM.

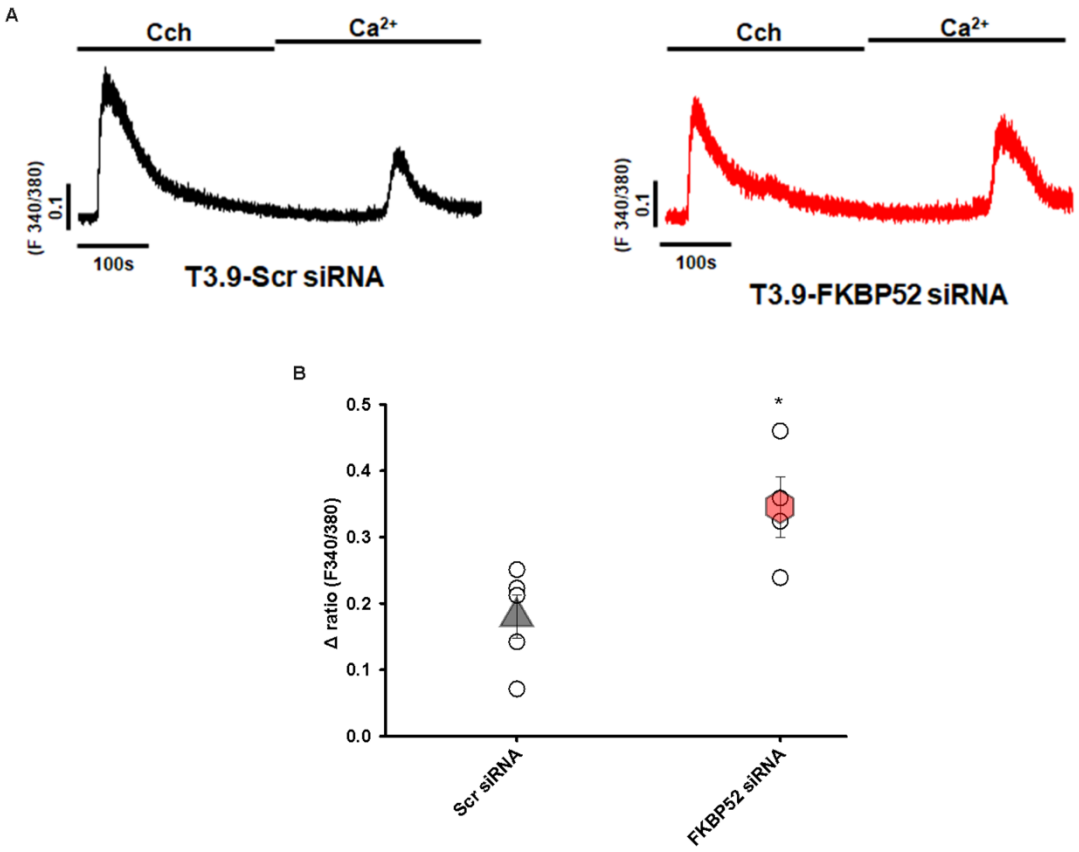

Fig. S6. TRPC3-dependent Ca^{2+} signals in HEK 293 cells are dependent on FKBP52. (A) Representative Ca^{2+} recordings of HEK 293 cells stably expressing TRPC3 (T3.9). The cells were treated with scramble (Scr siRNA) or FKBP52 siRNAs. A TRPC3-related Ca^{2+} influx was measured according to a classical Ca^{2+} re-addition protocol. T3.9 cells were first stimulated with the G_q protein-coupled receptor agonist carbachol (Cch, 300 µM) in nominally Ca^{2+}-free conditions and subsequently perfused with an external solution containing $CaCl_2$. This manoeuvre resulted in a Cch-dependent Ca^{2+} release from internal stores followed by a Ca^{2+} influx from the extracellular space. The TRPC3-mediated Ca^{2+} influx was significantly enhanced in cells treated with siRNAs against FKBP52. (B) Mean Δ ratio values were calculated by subtracting the peak value after Ca^{2+} re-addition from the baseline value *P<0.05 vs. Scr siRNA (unpaired t-test), *n* = 4-5, mean ± SEM. The mean Δ ratio of the Ca^{2+} release (peak-baseline) was not different between the groups. P= 0.34.